Doctoral dissertation

Zinc-dependent cytotoxicity of chemical compounds – Including a discussion of possible extension to environmental and regional sciences from cellular studies –

2017

Tomohiro Max Oyama

学位論文

化学物質の亜鉛イオン依存性細胞毒性 ― 細胞レベル研究から環境・地域科学への可能な展開についての考察を含めて ―

平成 29 年

小山 知博

本学位論文は以下の公刊された学術論文により構成される。

(1) Tomohiro M. Oyama, Keisuke Oyama, Toshihisa B. Oyama, Shiro Ishida, Yoshiro Okano, Yasuo Oyama
Zinc at clinically-relevant concentrations potentiates the cytotoxicity of polysorbate 80, a non-ionic surfactant.
Toxicology In Vitro 24 (2010) 737–744

(2) Tomohiro M. Oyama, Minoru Saito, Takayasu Yonezawa, Yoshiro Okano, Yasuo Oyama
Nanomolar concentrations of zinc pyrithione increase cell susceptibility to oxidative stress induced by hydrogen peroxide in rat thymocytes.
Chemosphere 87 (2012) 1316–1322

(3) Tomohiro M. Oyama, Shiro Ishida, Yoshiro Okano, Hakaru Seo, Yasuo Oyama
Clioquinol-induced increase and decrease in the intracellular Zn^{2+} level in rat thymocytes.
Life Sciences 91 (2012) 1216–1220

(4) Tomohiro M. Oyama, Keisuke Oyama, Eri Fukunaga, Hitoshi Ishibashi, Yasuo Oyama
Clioquinol, a lipophilic Zn^{2+} chelator, augments and attenuates the cytotoxicity of H_2O_2: a bell-shaped response curve of the effects of the drug
Toxicology Research 3 (2014) 110–117

Contents

Summary

It is well known that Ca^{2+} is deeply involved in various cellular functions. Maintaining intracellular Ca^{2+} homeostasis is vital, as changes in intracellular Ca^{2+} concentration triggers many physiological functions. The disruption of intracellular Ca^{2+} homeostasis can even induce pathological changes or cell death. Therefore, it is reasonable to correlate excessive elevations in intracellular Ca^{2+} concentration with the cytotoxicity of chemical substances. However, there is little information on metal ions other than Ca^{2+} with regard to the cytotoxicity of chemical substances. Micromolar levels of $ZnCl_2$ potentiate the cytotoxicity of hydrogen peroxide (H_2O_2) via the induction of oxidative stress while the chelator of intracellular Zn^{2+} completely attenuates the cytotoxicity of H_2O_2. It is necessary to examine the contribution of Zn^{2+} to the cytotoxicity of chemical compounds with applications in fields such as clinical practice and personal care. In this study, therefore, we first demonstrated that clinical concentrations of Zn^{2+} enhance the cytotoxicity of clinical levels of polysorbate 80, an injectable solubilizing agent, by increasing intracellular Zn^{2+} concentration. Secondly, we investigated the effect of an excessive increase in intracellular Zn^{2+} levels in cells especially vulnerable to oxidative stress by using zinc pyrithione, a Zn^{2+}-ionophore. Finally, we clarified the relationship between the expression of cytotoxicity and cytoprotection, and changes in intracellular Zn^{2+} concentration by clioquinol, a membrane-permeable Zn^{2+} chelator that is currently being investigated as a treatment for Alzheimer's disease. From these studies, we drew conclusions about the relationship between the cytotoxicity of chemical substances and changes in intracellular Zn^{2+} concentration, and further considered the significance of environmental science and regional science in our results.

(1) Polysorbate 80, a non-ionic surfactant, is used in the formula of water-insoluble anticancer agents for intravenous application. In our recent studies, this surfactant decreased cellular thiol content and the chemicals decreasing cellular thiol content increased intracellular Zn^{2+} concentration. In this study using rat thymocytes, the effect of polysorbate 80 on FluoZin-3 fluorescence, an indicator for intracellular Zn^{2+}, and the influence of $ZnCl_2$ on cytotoxicity of polysorbate 80 were examined in order to test the possibility that Zn^{2+} is involved in cytotoxic action of polysorbate 80. The surfactant at concentrations of 10 μg/ml or more significantly augmented FluoZin-3 fluorescent in a concentration-dependent manner, indicating an increase in intracellular Zn^{2+} concentration. The increase by polysorbate 80 was also observed after removing extracellular Zn^{2+}, suggesting an intracellular Zn^{2+} release. The simultaneous application of polysorbate 80 (30 μg/ml) and $ZnCl_2$ (10–30 μM) significantly increased cell lethality. The simultaneous application of $ZnCl_2$ accelerated the process of cell death induced by

polysorbate 80 and the combination increased oxidative stress. Results may indicate that the cytotoxicity of polysorbate 80 at clinical concentrations is modified by micromolar zinc. Although there is no clinical report that polysorbate 80 and zinc salt are simultaneously applied to human as far as our knowledge, it may be speculated that zinc induces some diverse actions in cancer treatment with water-insoluble anticancer agent including nanoparticle drug of which the solvent is polysorbate 80. (2) Zinc pyrithione is used as an antifouling agent. However, the environmental impacts of zinc pyrithione have recently been of concern. Zinc induces diverse actions during oxidative stress; therefore, we examined the effect of zinc pyrithione on rat thymocytes suffering from oxidative stress using appropriate fluorescent probes. The cytotoxicity of zinc pyrithione was not observed when the cells were incubated with 3 μM zinc pyrithione for 3 h. However, zinc pyrithione at nanomolar concentrations (10 nM or more) significantly increased the lethality of cells suffering from oxidative stress induced by 3 mM H_2O_2. The application of zinc pyrithione alone at nanomolar concentrations increased intracellular Zn^{2+} level and the cellular content of superoxide anions, and decreased the cellular content of nonprotein thiols. The simultaneous application of nanomolar zinc pyrithione and micromolar H_2O_2 synergistically increased the intracellular Zn^{2+} level. Therefore, zinc pyrithione at nanomolar concentrations may exert severe cytotoxic action on cells simultaneously exposed to chemicals that induce oxidative stress. (3) Clioquinol, a lipophilic Zn^{2+} chelator, has emerged as a potential novel therapeutic agent for several diseases such as cancer and Alzheimer's disease. Clioquinol has different effects on the intracellular Zn^{2+} concentrations in rat thymocytes, depending on its concentration and extracellular Zn^{2+} levels. In this study, we examined the effect of clioquinol on cells under oxidative stress induced by H_2O_2 by using a conventional flow cytometric technique with appropriate fluorescent probes. We observed a bell-shaped relationship between the clioquinol concentration and changes in H_2O_2 cytotoxicity; H_2O_2-induced cytotoxicity was the highest at a clioquinol concentration of 100 nM. Zn^{2+} chelators significantly decreased the clioquinol-induced increase in H_2O_2 cytotoxicity. A bell-shaped curve was observed between the increase in H_2O_2-induced cytotoxicity by clioquinol and the intracellular Zn^{2+} concentrations, although the maximal increases in Zn^{2+} levels were induced by 300 nM clioquinol. In addition, clioquinol at concentrations ≥100 nM exerted antioxidant activity by decreasing the cellular oxidant levels. Thus, clioquinol can exert pro-oxidant or antioxidant effects, depending on its concentration and the extracellular concentration of Zn^{2+}. Because of the unique Zn^{2+}-dependent effects and toxicological profile of clioquinol, clioquinol should be considered for clinical use.

As described above, the chemical has Zn^{2+}-dependent cytotoxicity, suggesting that the cytotoxicity of chemical substances is enhanced in the presence of Zn^{2+}. There are many chemical substances around us, and their cytotoxicity may develop because of coexistence with Zn^{2+}. The related concerns of note are as follows. Emissions from activities such as metal mining, inorganic pigment manufacturing, inorganic chemical industrial product manufacturing, surface-treated steel manufacturing, and electroplating, are a considerable source of environmental zinc exposure. According to the provisions in the Water Pollution Control Law in Japan, the permissible zinc levels of wastewater from business establishments are set at 2 mg/L or lower (calculated molar concentration: 30.6 μM). Zinc levels in river water of some countries are 2.1–301.3 μM. In our study, $ZnCl_2$ at 30 μM markedly potentiated the cytotoxicity of PS80 in vitro. The in vitro concentrations of $ZnCl_2$ are lower than the levels in river water, but they still potentiated the cytotoxicity of some chemical compounds. Thus, zinc is a critical factor that must be taken into consideration with regard to environmental conservation (or protection). It is necessary to consider the chemicophysical properties of compounds that may increase membrane Zn^{2+} permeability or form a membrane-permeable complex with Zn^{2+}. The concentration of zinc in the river water of Tokushima City is 0.005 mg/L, which is not a problematic level. However, the zinc concentration of river sediments varies depending on the geology and deposits in the area. Regional distribution of each element is shown in the geochemical map as important, basic, national information at the National Geological Survey Center of National Institute of Advanced Industrial Science and Technology. Therefore, it is necessary to manage chemical substances with zinc levels in river water and sediments in the future.

1. Introduction

While it is well-known now that Ca^{2+} is deeply involved in various cellular functions (Bootman et al., 2006; Iino, 2010), it was the role of Ca^{2+} in muscle contraction that was discovered first (Ebashi and Endo, 1968; Fye, 1984). The subsequent discovery of the Ca^{2+} receptor protein, calmodulin, also greatly progressed research on the role of Ca^{2+} in intracellular signaling (Kakiuchi and Yamazaki, 1970; Cheung, 1980). Maintaining intracellular Ca^{2+} homeostasis is vital, as changes in intracellular Ca^{2+} concentration triggers many physiological functions (Caafoli, 1987). The disruption of intracellular Ca^{2+} homeostasis can even induce pathological changes or cell death (Schanne et al., 1979). Many studies have shown that cytotoxic chemical substances, including organometallic compounds, induce an excessive increase in the intracellular Ca^{2+} concentration (Nicotera et al., 1992). Extracellular Ca^{2+} concentrations exceed intracellular concentrations by 10,000-fold or more, and changes in membrane ionic permeability induced by chemical substances can lead to an excessive increase in intracellular Ca^{2+} concentration. In addition, it is also well known that Ca^{2+} release from the endoplasmic reticulum (i.e., intracellular Ca^{2+} stores) by chemical substances causes Ca^{2+} depletion and subsequent store-operated Ca^{2+} influx (i.e., elevation of intracellular Ca^{2+} concentration) (Parekh and Penner, 1997; Smani et al., 2004). Therefore, it is reasonable to correlate excessive elevations in intracellular Ca^{2+} concentration with the cytotoxicity of chemical substances. However, there is little information on metal ions other than Ca^{2+} with regard to the cytotoxicity of chemical substances. We found that cell viability is markedly reduced by simultaneous incubation with clotrimazole (CTZ), an antifungal agent, and cadmium ($CdCl_2$), an environmental pollutant (Oyama et al., 2006). This was due to a CTZ-induced increase in membrane Cd^{2+} permeability (Oyama et al., 2007). As the experimental combination of CTZ and $CdCl_2$ is unusual, our process is briefly explained below. Horimoto et al. (2006) reported that CTZ suppressed Ca^{2+}-dependent cell death. Additionally, it has been suggested that Ca^{2+} is involved in the cytotoxicity of several heavy metals (Schanne et al., 1979). Thus, the possibility that CTZ suppresses cell death induced by $CdCl_2$ was considered. In the experiment described above, results rejecting this hypothesis were obtained (Oyama et al., 2006, 2007). The possibility that Zn^{2+} may be involved in the cytotoxicity of chemical substances, including pharmaceuticals, was suggested because Zn^{2+} and Cd^{2+} belong to the same category in the periodic table. In fact, it has been reported that a combination of imidazole antifungals (including CTZ) and $ZnCl_2$ markedly reduced cell viability, with antifungals markedly increasing membrane Zn^{2+} permeability (Matsui et al., 2008). Furthermore, micromolar levels

of $ZnCl_2$ have been found to potentiate the cytotoxicity of hydrogen peroxide (H_2O_2) via the induction of oxidative stress (Matsui et al., 2010). It is necessary to examine the contribution of Zn^{2+} to the cytotoxicity of chemical compounds with applications in fields such as clinical practice and personal care. Therefore, we first demonstrated that clinical concentrations of Zn^{2+} enhance the cytotoxicity of clinical levels of polysorbate 80, an injectable solubilizing agent, by increasing intracellular Zn^{2+} concentration (Oyama et al., 2010). Secondly, we investigated the effect of an excessive increase in intracellular Zn^{2+} levels in cells especially vulnerable to oxidative stress by using zinc pyrithione, a Zn^{2+}-ionophore (Oyama et al., 2012). Finally, we clarified the relationship between the expression of cytotoxicity and cytoprotection, and changes in intracellular Zn^{2+} concentration by clioquinol, a membrane-permeable Zn^{2+} chelator that is currently being investigated as a treatment for Alzheimer's disease (Oyama et al., 2012, 2014). From these studies, we drew conclusions about the relationship between the cytotoxicity of chemical substances and changes in intracellular Zn^{2+} concentration, and further considered the significance of environmental science and regional science in our results.

2. Materials and Methods

2.1. Chemicals

2.1.1. Chemicals – PS80 study

Polysorbate 80 was purchased from Wako Pure Chemicals (Osaka, Japan). Chelators for Zn^{2+}, diethylenetriamine-N,N,N',N'',N''-pentaacetic acid (DTPA) and N,N,N',N'-tetrakis(2-pyridylmethyl)ethylenediamine (TPEN), were obtained from Dojin Chemical Laboratory (Kumamoto, Japan). Fluorescent probes, annexin V-fluorescein isothiocianate (annexin V-FITC), propidium iodide, FluoZin3-pentaacetoxymethyl ester (FluoZin3-AM), dihydroethidium, 5-chloromethylfluorescein diacetate (5-CMF-DA), and 5-(and-6)-carboxy-2',7'-dichlorofluorescin diacetate (DCFH-DA) were the products of Molecular Probes Inc. (Eugene, Oregon, USA). NaCl, $MgCl_2$, KCl, glucose, HEPES, NaOH, $ZnCl_2$, and dimethyl sulfoxide (DMSO) were also purchased from Wako Pure Chemicals. Final concentration of DMSO as a solvent for TPEN, FluoZin3-AM, DCFH-DA and 5-CMF-DA in cell suspension was 0.3 % or less. The incubation with DMSO at 0.3 % or less did not affect the viability of rat thymocytes during experiments.

2.1.2. Chemicals – ZP study

Zinc pyrithione, NaCl, $CaCl_2$, $MgCl_2$, KCl, glucose, HEPES, NaOH, dimethyl sulfoxide (DMSO) and H_2O_2 were obtained from Wako Pure Chemicals (Osaka, Japan). Zinc chelator,

N,N,N',N'-tetrakis[2-pyridylmethyl]ethylenediamine (TPEN), was obtained from Dojin Chemical Laboratory (Kumamoto, Japan). FluoZin-3-AM, 5-chloromethylfluorescein diacetate (5-CMF-DA), dihydroethidium and propidium iodide were products of Molecular Probes Inc. - Invitrogen (Eugene, Oregon, USA). Zinc pyrithione, TPEN, FluoZin-3-AM, 5-CMF-DA, and dihydroethidium were initially dissolved with DMSO. Final concentration of DMSO in cell suspension (0.2% or less) did not affect fluorescence and cell viability.

2.1.3. Chemicals – CQ study

Clioquinol was purchased from Biolmol/Enzo Life Sciences Inc. (Farmingdale, NY, USA). The purity of clioquinol was 98% (Thin-layer chromatography, 5% methanol/methylene chloride + 0.5% NH_4OH; Rf = 0.25). Clioquinol was initially dissolved in dimethyl sulfoxide (DMSO) just before use. Subsequently, the DMSO solution was added to the cell suspension. The final concentration of DMSO was 0.1%. The viability of rat thymocytes did not change after treatment with 0.3% DMSO.

NaCl, $CaCl_2$, $MgCl_2$, KCl, glucose, HEPES, NaOH, DMSO, and H_2O_2 were obtained from Wako Pure Chemicals (Osaka, Japan). The Zn^{2+} chelators diethylenetriamine-N,N,N',N'',N''-pentaacetic acid (DTPA) and N,N,N',N'-tetrakis(2-pyridylmethyl)ethylenediamine (TPEN) were obtained from Dojin Chemical Laboratory (Kumamoto, Japan). FluoZin-3-AM, propidium iodide, 5-(and-6)-chloromethyl-2',7'-dichlorodihydrofluorescein diacetate (CM-H_2DCF-DA), and 5-chloromethylfluorescein diacetate (5-CMF-DA) were obtained from Molecular Probes Inc. Invitrogen (Eugene, OR, USA).

2.2. Animals and cell preparation

This study was approved by the Committee for Animal Experiments in the University of Tokushima (No. 05279).

The procedure to prepare cell suspension was similar to that previously reported (Chikahisa and Oyama, 1992; Chikahisa et al., 1996). In brief, thymus glands dissected from ether-anesthetized rats (Wistar strain, Charles River Laboratories, Yokohama, Japan) were sliced at a thickness of 400-500 μm with razor under an ice-cold condition (1-4ºC). We chose Wistar strain because it is currently one of the most popular rat strains used for laboratory research and both Sprague Dawley rat and Long-Evans rat strains were developed from Wistar rats. The slices of thymus glands were triturated by gently shaking in chilled normal Tyrode's solution (in mM: NaCl 150, KCl 5, $CaCl_2$ 2, $MgCl_2$ 1, glucose 5, HEPES 5, with an appropriate amount of NaOH to adjust pH to 7.3-7.4) or Ca^{2+}-free Tyrode's solution (in mM: NaCl 150, KCl

5, $MgCl_2$ 3, glucose 5, HEPES 5, with an appropriate amount of NaOH to adjust pH to 7.3-7.4) to dissociate thymocytes. Thereafter, Tyrode's solution containing the cells was passed through a mesh (a diameter of 10 μm) to prepare the cell suspension (about 5×10^5 cells/ml). The beaker containing the cell suspension was water-bathed at 36ºC for 1 h at least before the experiment. Twenty-five rats were used in this study. Each experiment was carried out with the cells obtained a single animal. Each result was obtained from four experiments at least.

Thymocyte is used for a model experiment of cytotoxicity induced by chemical compounds because of following reasons. First, cell membranes are remained intact because single cells are prepared without any enzymatic treatment. Second, several types of hormones, biological compounds, and chemicals induce cell death including apoptosis in thymocytes (Quaglino and Ronchetti, 2001). Especially, polysorbate 80 is used as a solvent for some anticancer agents. Some agents increase the incidence of thymus atrophy (Choyke et al., 1987; Hendrickx and Dohring, 1989; Chung et al., 2006; Gruver and Sempowski, 2008). Third, the process of cell death in thymocytes is well defined (McConkey et al., 1994).

2.3. Experimental protocol

2.3.1. Experimental protocol – PS80 study

Polysorbate 80, $ZnCl_2$, and their combination were respectively added to the cell suspension (2 ml cell suspension in each 10 ml test tube). To examine the effects of zinc-chelators, respective chelator was added to the suspension at 1-2 min before applying polysorbate 80, $ZnCl_2$, or their combination. The cells were incubated with the agent(s) at 36 °C under room air condition. The incubation time was dependent on each experimental purpose. The data acquisition of fluorescence from 2500 cells by a flow cytometer required 30 sec at maximum.

2.3.2. Experimental protocol – ZP study

H_2O_2 (2 μL) was added to the cell suspension (2 mL). The cell density was about 5×10^5 cells/mL. To examine the effect of zinc pyrithione, the agent was added to the suspension just before applying H_2O_2. The cells were incubated with zinc pyrithione and H_2O_2 at 36–37 °C. The data acquisition of fluorescence from 2×10^3 cells by a flow cytometer required at least 10 s. Effect of H_2O_2 at concentrations of 1, 3, and 10 mM on thymocytes has been examined in previous studies (Nagano et al., 1997; Matsui et al., 2009). Thymocytes were tolerant to the oxidative stress induced by 1 mM H_2O_2 during a period of 3 h after adding H_2O_2 to cell suspensions. However, it was likely that H_2O_2 at 3–10 mM was lethal for thymocytes during exposure lasting 2 h or longer because prolonged exposure of thymocytes to 3 mM H_2O_2

produced a time-dependent increase in the number of dead cells and/or cells having compromised membranes. The time-dependent change in the cell lethality (or the population of cells with propidium fluorescence) in the presence of 10 mM H_2O_2 was more rapid than that in the presence of 3 mM H_2O_2. The incubation with 10 mMH2O2 for 2 h ensured a large increase (more than 40%) in cell lethality that was suitable to examine the protective action of the agent against oxidative stress induced by H_2O_2. On the other hand, incubation with 3 mM H_2O_2 for 2 h induced a small increase (10–20%) in cell lethality that was suitable to examine the potentiation.

2.3.3. Experimental protocol – CQ study

Clioquinol (2 μL in DMSO) was added at various concentrations to cell suspensions (2 mL). The cell density was approximately 5×10^5 cells/mL. The acquisition of fluorescence data by using flow cytometry from 2×10^3 cells required at least 10 s. Oxidative stress was induced by 300 μM H_2O_2. Cell death in rat thymocyte suspensions under control conditions was 5–6% and did not change during the experiment (4 h), while incubation with 300 μM H_2O_2 for 3–4 h increased the rate of cell death to 10–20%. The cells incubated with 300 μM H_2O_2 for 3–4 h completely depleted cellular glutathione (Chikahisa et al., 1996). FluoZin-3 fluorescence was monitored at 2 h after applications of clioquinol alone, H_2O_2 alone, and their combination because the peak response was obtained within 2 h after the application.

2.4. Fluorescence measurements of cellular and membrane parameters

2.4.1. Measurements – PS80 study

The methods for measurements of cellular and membrane parameters using a flow cytometer equipped with an argon laser (CytoACE-150, JASCO, Tokyo, Japan) and fluorescent probes were similar to those previously described (Chikahisa and Oyama, 1992; Chikahisa et al., 1996; Matsui et al., 2008). The fluorescence was analyzed by JASCO software (Ver.3XX, JASCO). From chemicals, except for fluorescent probes, used in this study, there was no fluorescence under our experimental condition.

To assess cell lethality, propidium iodide was added to cell suspension to achieve a final concentration of 5 μM. Since propidium stains dead cells, the measurement of propidium fluorescence from cells provides a clue to estimate the lethality. The fluorescence was measured at 2 min after the application of propidium iodide by a flow cytometer. Excitation wavelength for propidium was 488 nm and emission was detected at 600 ± 20 nm.

FluoZin-3-AM (Gee et al., 2002) was used as an indicator for intracellular Zn^{2+}. The cells were incubated with 500 nM FluoZin-3-AM for 60 min before any fluorescence

measurements to estimate the change in intracellular Zn^{2+} concentration of rat thymocytes with intact membranes. FluoZin-3 fluorescence was measured from the cells that were not stained with 5 μM propidium iodide (Matsui et al., 2008). Excitation wavelength for FluoZin-3 was 488 nm and emission was detected at 530 ± 20 nm.

5-CMF-DA was used to monitor the change in cellular content of nonprotein thiols (Chikahisa et al., 1996). The cells were incubated with 1 μM 5-CMF-DA for 30 min before any fluorescence measurements. 5-CMF fluorescence was measured from the cells that were not stained with 5 μM propidium iodide. Excitation wavelength for 5-CMF was 488 nm and emission was detected at 530 ± 15 nm.

Dihydroethidium and DCFH-DA were used to detect intracellular reactive oxygen species. The cells were respectively incubated with dihydroethidium and DCFH-DA at 10 μM for 60 min before any fluorescence measurement. Excitation wavelength was 488 nm and emissions were detected at 530 ± 20 nm for DCFH-DA experiment and at 600 ± 15 nm for dihydroethidium experiment.

The exposure of phosphatidylserine on outer thymocyte membranes was detected by using annexin V-FITC and propidium iodide (Nakata et al., 1999, Oyama et al., 1999). The excitation wavelength for the fluorescent dyes was 488 nm. The emissions were detected at 530 ± 20 nm for FITC (annexin V binding to membranes) and 600 ± 20 nm for propidium iodide.

2.4.2. Measurements – ZP study

The methods for measurements of cellular and membrane parameters using a flow cytometer equipped with an argon laser (CytoACE-150; JASCO, Tokyo, Japan) and fluorescent probes were similar to those previously described (Chikahisa et al., 1996; Matsui et al., 2008). The fluorescence was analyzed by JASCO software (Version 3.06; JASCO). There was no fluorescence from reagents used in this study, except for fluorescent probes, under our experimental conditions.

To assess cell lethality, propidium iodide was added to cell suspensions to achieve a final concentration of 5 μM. Because propidium stains dead cells, the measurement of propidium fluorescence from cells provides information regarding lethality. The fluorescence was measured 2 min after the application of propidium iodide by a flow cytometer. The excitation wavelength for propidium was 488 nm and emission was detected at 600 ± 20 nm.

FluoZin-3-AM (Gee et al., 2002) was used as an indicator for intracellular Zn^{2+}. The cells were incubated with 500 nM FluoZin-3-AM for 60 min before any fluorescence

measurements to estimate the change in intracellular Zn^{2+} level of rat thymocytes with intact membranes. FluoZin-3 fluorescence was measured in the cells that were not stained with 5 μM propidium iodide (Matsui et al., 2008). The excitation wavelength for FluoZin-3 was 488 nm and emission was detected at 530 ± 20 nm.

5-CMF-DA was used to monitor the change in cellular content of nonprotein thiols (Chikahisa et al., 1996). The cells were incubated with 1 μM 5-CMF-DA for 30 min before any fluorescence measurements. 5-CMF fluorescence was measured in the cells that were not stained with 5 μM propidium iodide. The excitation wavelength for 5-CMF was 488 nm and emission was detected at 530 ± 15 nm.

Dihydroethidium was used to detect intracellular superoxide anions (Fink et al., 2004). The cells were incubated with 10 μM dihydroethidium for 60 min before any fluorescence measurement. The excitation wavelength was 488 nm and emission was detected at 600 ± 15 nm.

2.4.3. Measurements – CQ study

The methods for measuring the cellular and membrane parameters using a flow cytometer equipped with an argon laser (CytoACE-150; JASCO, Tokyo, Japan) and fluorescent probes were similar to those previously described (Chikahisa et al., 1996; Matsui et al., 2008). Fluorescence was analyzed using the JASCO software (Version 3.06; JASCO, Tokyo, Japan). Under our experimental conditions, no fluorescence was observed from the reagents used in the study, except from the fluorescent probes.

To assess cell death, propidium iodide was added to the cell suspensions at a final concentration of 5 μM. Propidium iodide only stains dead cells, and thus measurement of the intensity of propidium iodide fluorescence is an indicator of cell death. Fluorescence was measured using flow cytometry 2 min after application of propidium iodide. The excitation wavelength used for measuring the fluorescence of propidium iodide was 488 nm and the emission wavelength was 600 ± 20 nm.

FluoZin-3-AM was used as an indicator of intracellular Zn^{2+} levels (Gee et al., 2002). Cells were incubated with 500 nM FluoZin-3-AM for 60 min before fluorescence measurements were performed to estimate the changes in the intracellular Zn^{2+} concentrations in rat thymocytes with intact membranes. FluoZin-3 fluorescence was measured in cells that were not stained with propidium iodide (Matsui et al., 2008). The excitation wavelength used to determine FluoZin-3 fluorescence was 488 nm and the emission wavelength was 530 ± 20 nm.

CM-H_2DCF-DA was used to determine the cellular oxidant levels (Koopman et al., 2007).

Cells were incubated with 3 μM CM-H_2DCF-DA for at least 30 min before fluorescence measurements were performed. Fluorescence (CM-DCF fluorescence) after cellular hydrolysis and oxidation of CM-H_2DCF-DA was monitored in cells with intact membranes. The excitation wavelength used to determine CM-DCF fluorescence was 488 nm and the emission wavelength was 530 ± 20 nm.

2.5. Statistics

Values were expressed as the mean ± standard deviation of 4 experiments. Statistical analysis was performed by using Tukey multivariate analysis. A P value of < 0.05 was considered significant.

3. Results

3.1. PS80 study

3.1.1. Increase in the intensity of FluoZin-3 fluorescence by polysorbate 80

Polysorbate 80 at 10 μg/ml or more increased the intensity of FluoZin-3 fluorescence in a time-dependent manner and the action reached a steady-state level within 1 h. As shown in Fig. 1, the incubation of cells with polysorbate 80 at 10 and 30 μg/ml for 1 h shifted the histogram of FluoZin-3 fluorescence to a direction of higher intensity while it was not the case for 3 μg/ml0. Concentration-dependent change in the intensity of FluoZin-3 fluorescence by polysorbate 80 at concentrations ranging from 1 μg/ml to 300 μg/ml is summarized in Fig. 2. Polysorbate 80 at 10 μg/ml started to significantly increase the intensity. Further increase in the concentration (up to 100 μg/ml) induced further significant increase in the intensity. The increase in fluorescence by 300 μg/ml was similar to that by 100 μg/ml. From the results described above, it is suggested that polysorbate 80 at concentrations of 10 μg/ml or more increases intracellular Zn^{2+} concentration.

Figure 1

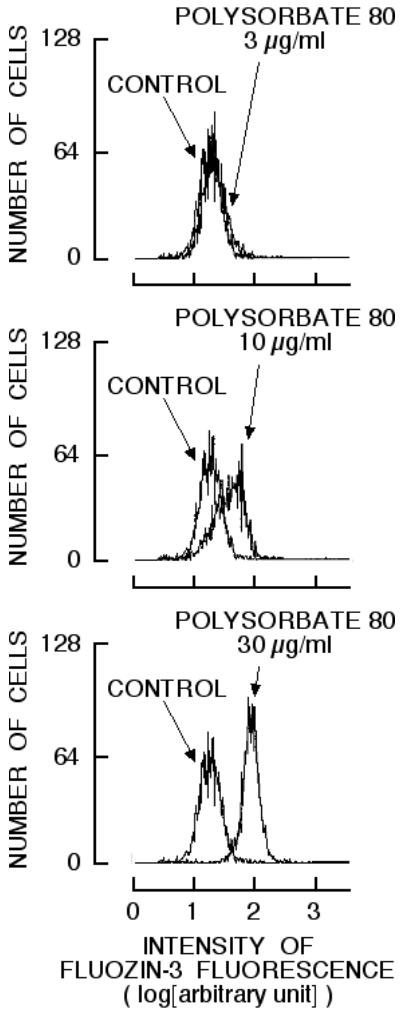

Fig. 1. Effect of polysorbate 80 on FluoZin-3 fluorescence of rat thymocytes. The histogram of FluoZin-3 fluorescence was constructed with 2000 cells. Effect was examined at 1 h after the start of application. It is noted that the shift of histogram to a direction of higher intensity of FluoZin-3 fluorescence indicates an increase in intracellular Zn^{2+} concentration.

Figure 2

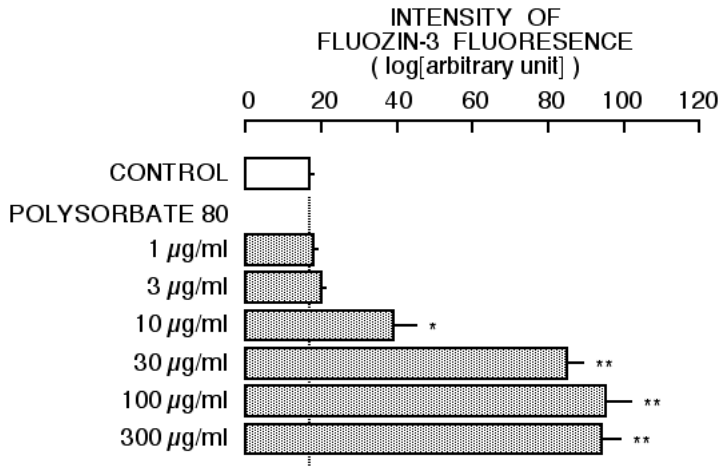

Fig. 2. Concentration-dependent augmentation of FluoZin-3 fluorescence by polysorbate 80 at concentrations ranging from 1 μg/ml to 300 μg/ml. Column and bar indicate mean intensity and its standard deviation of four experiments, respectively. Asterisks (*, **) show significant difference ($P < 0.05$, $P < 0.01$) between control group (CONTROL) and the group of cells treated with polysorbate 80 (POLYSORBATE 80)

3.1.2. Effects of Zn^{2+}-chelators and $ZnCl_2$ on the augmentation of FluoZin-3 fluorescence by polysorbate 80

To examine the source of Zn^{2+} for the augmentation of FluoZin-3 fluorescence by polysorbate 80, the effects of Zn^{2+}-chelators, DTPA and TPEN, were tested. The incubation with 10 μM TPEN, a chelator for extra- and intracellular Zn^{2+}, completely diminished the augmentation of FluoZin-3 fluorescence by 30 μg/ml polysorbate 80 (Fig. 3). Thus, it is suggested that the augmentation by polysorbate 80 is dependent on Zn^{2+}. In the presence of 10 μM DTPA, a chelator for extracellular Zn^{2+}, polysorbate 80 at 30 μg/ml significantly increased the intensity of FluoZin-3 fluorescence (Fig. 3), suggesting that the release of intracellular Zn^{2+} is involved in the augmentation of FluoZin-3 fluorescence by polysorbate 80. However, the degree of augmentation of FluoZin-3 fluorescence by polysorbate 80 in the presence of DTPA was lower than that in the absence of DTPA. The cells suspension contained Zn^{2+} derived from cell preparation although the Tyrode's solution was prepared without $ZnCl_2$ (Sakanashi et al., 2009). Thus, it cannot be ruled out the possibility that polysorbate 80 at 30 μg/ml increases membrane Zn^{2+} permeability, resulting in the influx of Zn^{2+}. Therefore, the effect of

extracellularly-applied $ZnCl_2$ was tested. As shown in Fig. 3, in the presence of 10 μM $ZnCl_2$, polysorbate 80 at 30 μg/ml significantly and further increased the intensity of FluoZin-3 fluorescence although the base level of FluoZin-3 fluorescence was greatly increased. It is suggested that polysorbate 80 at 30 μg/ml increases membrane Zn^{2+} permeability.

Figure 3

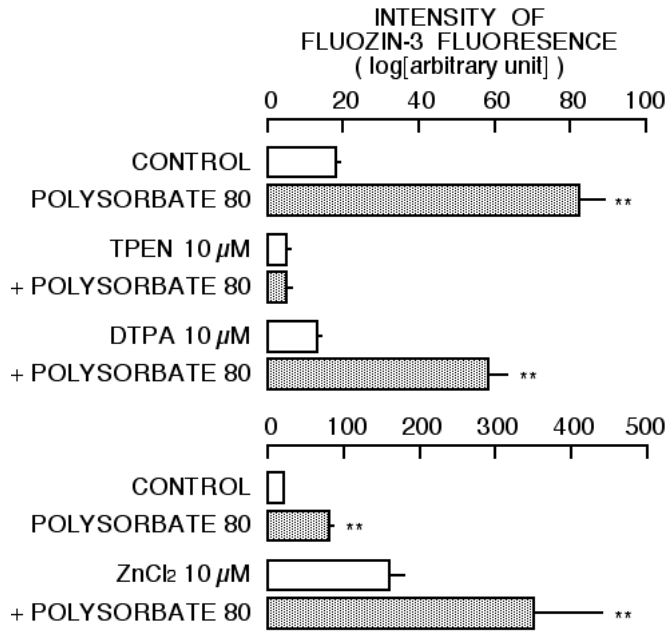

Fig. 3. Effects of polysorbate 80 on FluoZin-3 fluorescence in presence of TPEN, DTPA, and $ZnCl_2$. Column and bar show mean intensity and its standard deviation, respectively, of four experiments. Asterisk (**) indicates significant difference ($P < 0.01$) between paired columns in absence and presence of polysorbate 80.

3.1.3. Effects of extracellularly-applied $ZnCl_2$ on the cytotoxicity induced by polysorbate 80

It is likely that polysorbate 80 at 30 μg/ml increases membrane Zn^{2+} permeability and releases intracellular Zn^{2+}, resulting in the increase in intracellular Zn^{2+} concentration. To see if the increase in intracellular Zn^{2+} concentration modifies the cytotoxicity of polysorbate 80, the effect of extracellularly-applied $ZnCl_2$ was tested. As shown in Fig. 4, the incubation of cells with 30 μM $ZnCl_2$ or 30 μg/ml polysorbate 80 for 3 h slightly increased the population of cells exerting propidium fluorescence. On the other hand, the simultaneous application of $ZnCl_2$ and polysorbate 80 greatly increased the population (Fig. 4). Effect of $ZnCl_2$ at

concentrations ranging from 10 μM to 100 μM on the cytotoxicity of 30 μg/ml polysorbate 80 is summarized in Fig. 5. The incubation time with $ZnCl_2$, polysorbate 80, or their combination was 3 h. The time-dependent increase in the population of cells exerting propidium fluorescence was observed in the case of simultaneous application of polysorbate 80 and $ZnCl_2$ during the incubation. While $ZnCl_2$ alone at concentrations ranging from 10 μM to 100 μM increased the population only by 10 % or less, $ZnCl_2$ greatly augmented the cytotoxicity of polysorbate 80 in a concentration-dependent manner (Fig. 5). In the case of 30 μg/ml polysorbate 80 with 100 μM $ZnCl_2$, the population of cells exerting propidium fluorescence was 90.5 ± 4.4 % (mean ± SD of 4 experiments).

Figure 4

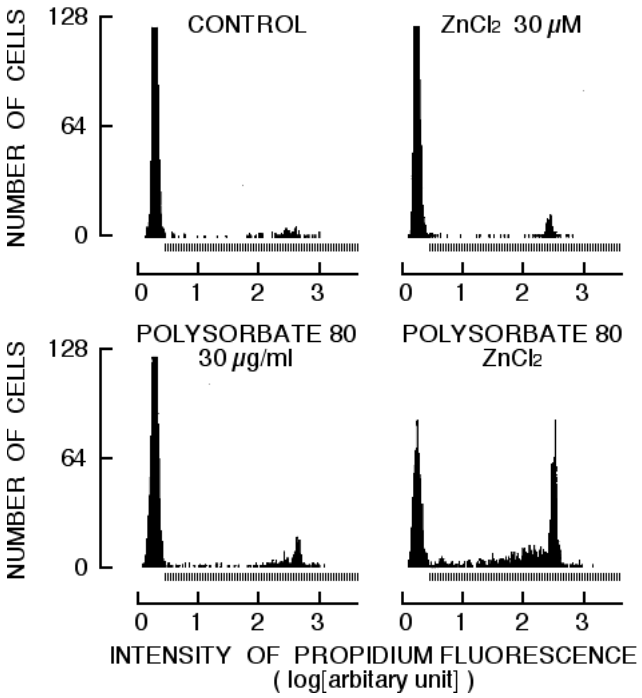

Fig. 4. The histograms of propidium fluorescence monitored from the cells treated with $ZnCl_2$, polysorbate 80, and their combination. The histogram was obtained at 3 h after the start of respective application. The line under histogram shows the cells exerting propidium fluorescence, presumably dead cells or the cells with compromised membranes. The histogram was constructed with 2000 cells.

Figure 5

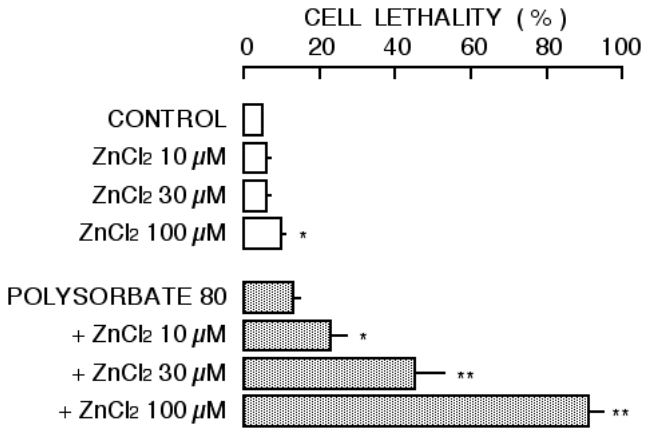

Fig. 5. Effect of $ZnCl_2$ on the cell lethality of rat thymocytes in absence (upper panel) and presence (lower panel) of polysorbate 80. Column and bar respectively indicate mean lethality and its standard deviation of four experiments. Asterisks (*, **) respectively indicate significant difference ($P < 0.05$, $P < 0.01$) between respective control and $ZnCl_2$-treated group.

3.1.4. Type of cell death induced by simultaneous application of $ZnCl_2$ and polysorbate 80

The increase in population of cells exerting propidium fluorescence by simultaneous application of polysorbate 80 and $ZnCl_2$ was associated with the increase in population of shrunken cells (Fig. 6). Cell shrinkage is one of parameters during early stage of apoptosis (Klassen et al., 1993; Beauvais et al., 1995; Bortner and Cidlowski, 1998). To confirm an externalization of phosphatidylserine that is also a parameter for early stage of apoptosis, the cells were incubated with annexin V-FITC. The cells with phosphatidylserine exposed on outer surface of membranes become annexin V-positive cells exerting FITC fluorescence. The incubation of cells with polysorbate 80 at 30 μg/ml for 2 h significantly increased the populations of annexin V-positive living cells (area A in Fig. 7). The incubation time was 2 h for the experiment using annexin V-FITC because further incubation induced great decrease in cell viability (Fig. 5). The combination of polysorbate 80 with 30 μM $ZnCl_2$ greatly increased the populations of annexin V-positive living cells and annexin V-positive cells exerting propidium fluorescence, dead cells (area AP in Fig. 7), resulting in the decrease in population of intact living cells (area N in Fig. 7). Results are summarized in Fig. 8. The combination of polysorbate and $ZnCl_2$ induced profound increase in population of annexin V-positive living

cells when the incubation time was 2 h. Increase in intracellular Zn^{2+} concentration may prompt the process of apoptotic cell death induced by polysorbate 80. However, the population of cells containing hypodiploid DNA in simultaneous presence of 30 μg/ml polysorbate 80 and 30 μM $ZnCl_2$ was less than 5 % (not shown) while that of cells exerting propidium fluorescence, dead cells, was more than 40 % (Fig. 8). Thus, main type of cell death by the combination of polysorbate 80 and $ZnCl_2$ seems to be necrosis with some apoptotic characteristics.

(Figures 6, 7, and 8 near here)

Figure 6

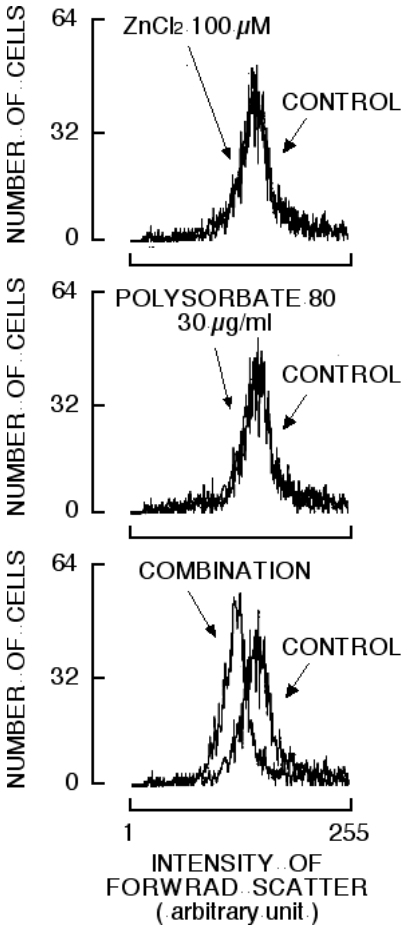

Fig. 6. Effects of polysorbate 80, $ZnCl_2$, and their combination on the intensity of forward scatter of rat thymocytes. The histogram was constructed with 2000 cells. The effect was examined at 2 h after the start of application.

Figure 7

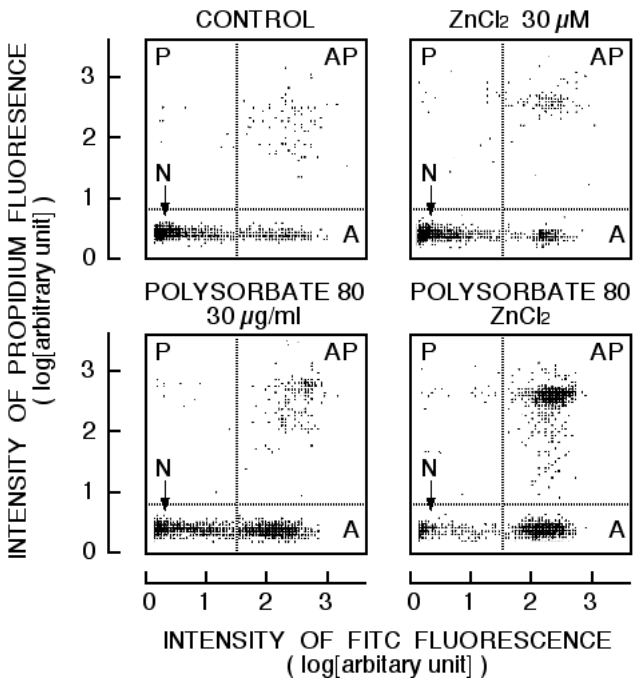

Fig. 7. Effects of $ZnCl_2$, polysorbate 80, and their combination on fluorescence cytogram (propidium fluorescence versus FITC fluorescence) of rat thymocytes. The cytogram, constructed with 2000 cells, consisted of four populations (P: the cells exerting only propidium fluorescence, AP: the cells exerting both propidium and FITC fluorescence, N: the cells without propidium and FITC fluorescence, A: the cells exerting only FITC fluorescence).

Figure 8

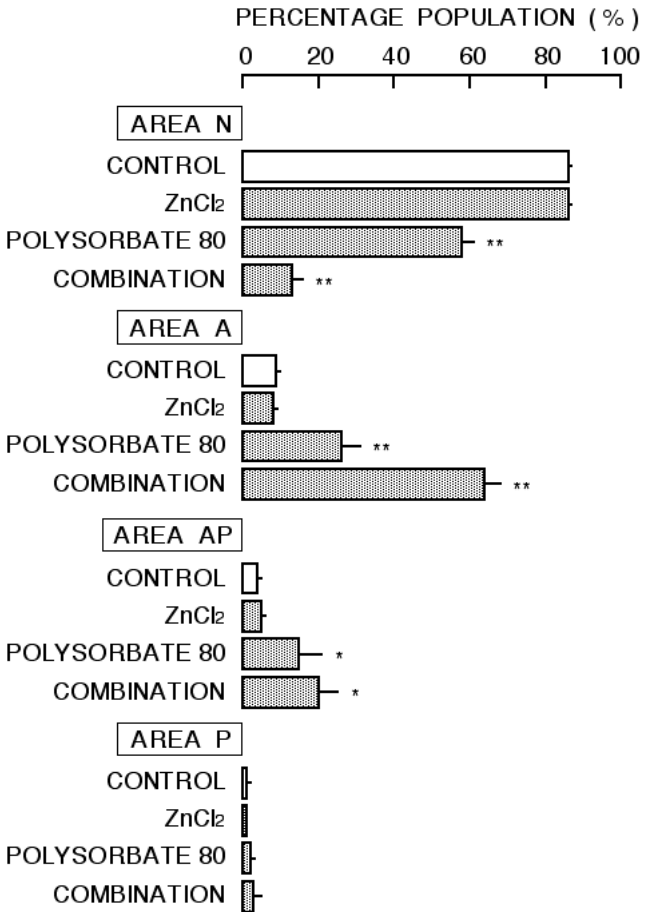

Fig. 8. The populations of cells incubated with $ZnCl_2$, polysorbate 80, and their combination. Column and bar respectively indicate mean population and its standard deviation of four experiments. Asterisks (*, **) respectively indicate significant difference ($P < 0.05$, $P < 0.01$) to respective control.

3.1.5. Possible mechanism of cell death induced by simultaneous application of $ZnCl_2$ and polysorbate 80

Polysorbate 80 at concentrations ranging from 10 μg/ml to 300 μg/ml decreased the intensity of 5-CMF fluorescence, a fluorescent indicator for cellular thiol content (Hirama et al., 2004). In our recent study (Matsui et al., 2009), $ZnCl_2$ at 10 μM significantly increased the population of dead cells induced by 10 mM hydrogen peroxide. If polysorbate 80 induces oxidative stress, $ZnCl_2$ would potentiate the cytotoxicity induced by hydrogen peroxide. First

of all, we examined the effects of $ZnCl_2$, polysorbate 80, and their combination on 5-CMF fluorescence. As shown in Fig. 9A, $ZnCl_2$ at 30 μM significantly increased the intensity of 5-CMF fluorescence, suggesting the zinc-induced increase in cellular thiol content. It may be common because zinc has been reported to increase cellular glutathione content (Farinati et al., 2003; Ha et al., 2006; Cortese et al., 2008). However, polysorbate 80 at 30 μg/ml greatly decreased the intensity of 5-CMF fluorescence in absence and presence of 30 μM $ZnCl_2$. To see if polysorbate 80 elevates cellular levels of reactive oxygen species in absence and presence of external $ZnCl_2$, the effects of 30 μg/ml polysorbate 80, 30 μM $ZnCl_2$, and their combination were compared in the cells incubated respectively with dihydroethidium and DCFH-DA. As shown in Fig. 9B, the incubation of cells with 30 μg/ml polysorbate 80 for 3 h significantly increased both intensities of fluorescence monitored from the cells and simultaneously-applied $ZnCl_2$ (30 μM) further augmented the fluorescence's. Thus, $ZnCl_2$ may further increase the oxidative stress induced by polysorbate 80.

Figure 9

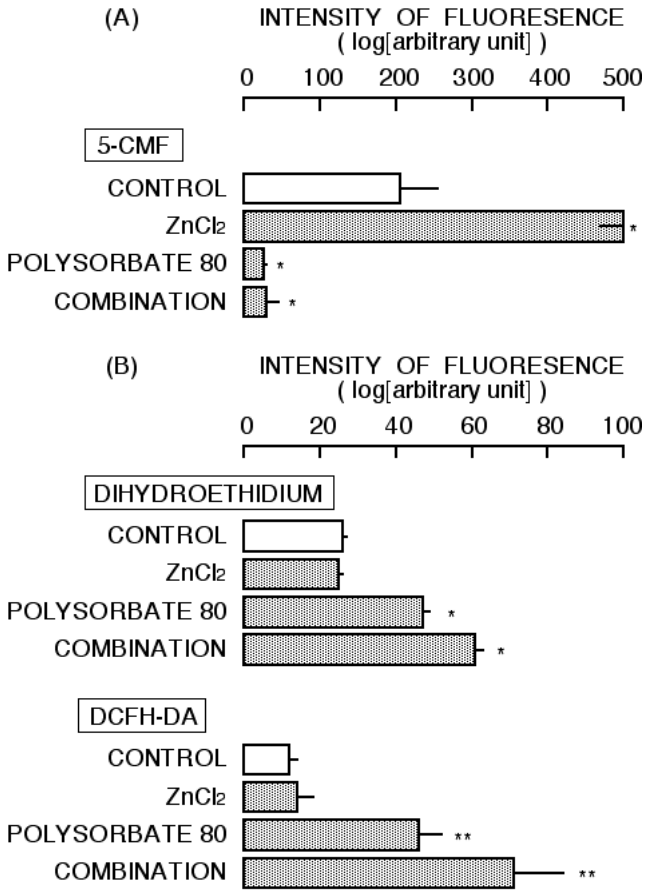

Fig. 9. Effects of $ZnCl_2$, polysorbate 80, and their combination on the fluorescence monitored from the cells incubated respectively with 5-CMF-DA (A), dihydropropidium (B upper), and DCFH-DA (B lower). Column and bar indicate mean intensity and its standard deviation of four experiments. Asterisks (*, **) respectively indicate significant difference ($P < 0.05$, $P < 0.01$) to respective control.

3.1.6. Effect of curcumin, a potent antioxidant agent, on the lethality increased by the combination of polysorbate 80 and $ZnCl_2$

Curcumin is a potent antioxidant (Menon and Sudheer, 2007; Ak and Gülçin, 2008). We examined the effect of curcumin on the lethality increased by the combination of polysorbate 80 and $ZnCl_2$ to support the possible involvement of oxidative stress. However, the treatment with 3 μM curcumin did not attenuate the increase in cell lethality induced by the combination (Fig. 10) although the concentration (3 μM) of curcumin was sufficient to reduce

the cell lethality increased by 3 mM hydrogen peroxide (Oyama et al., 1998).

Figure 10

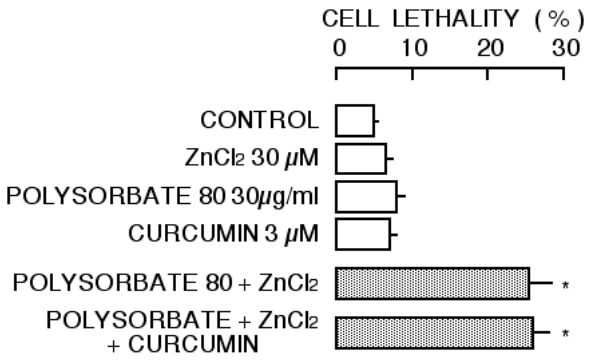

Fig. 10. Effect of curcumin on the lethality increased by the combination of polysorbate 80 and $ZnCl_2$. Column and bar indicate mean intensity and its standard deviation of four experiments. Asterisk (*) indicates significant difference ($P < 0.05$) to the control.

Figure 11

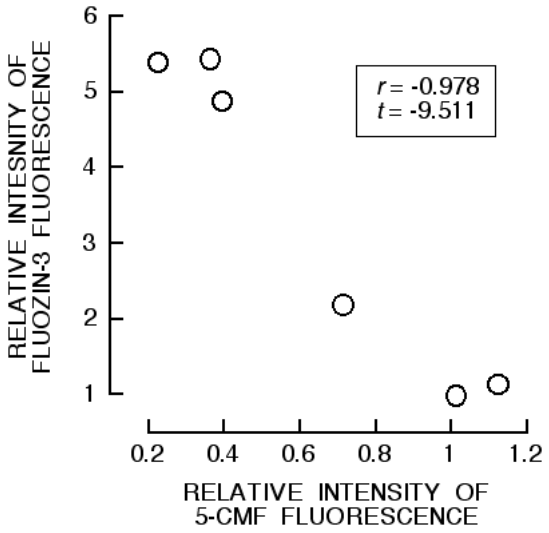

Fig. 11. The relation between the changes in FluoZin-3 and 5-CMF fluorescence by polysorbate 80 at concentrations ranging from 1 μg/ml to 300 μg/ml.

Figure 12

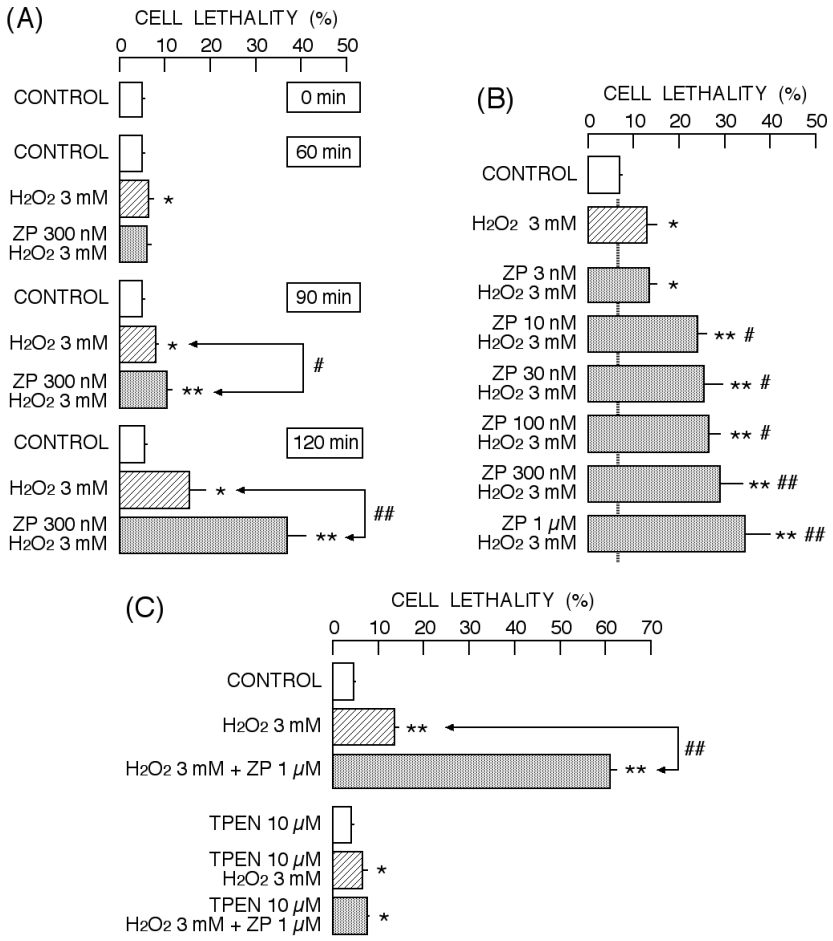

Fig. 12. Change in cell lethality by zinc pyrithione. Columns and bars respectively indicate mean and standard deviation of 4 experiments. Symbols (*, **) show significant differences ($P < 0.05$, $P < 0.01$) between control group and respective test groups. (A) Time-dependent change in cell lethality by 300 nM zinc pyrithione (ZP), 3 mM H_2O_2, and their combination. Symbols ($^{\#}$, $^{\#\#}$) indicate significant differences ($P < 0.05$, $P < 0.01$) between paired groups. (B) Concentration-dependent change in cell lethality by zinc pyrithione in the presence of H_2O_2. Effects were examined 2 h after the start of simultaneous application. Symbols ($^{\#}$, $^{\#\#}$) indicate significant differences ($P < 0.05$, $P < 0.01$) between the group of cells treated with 3 mM H_2O_2 and respective test groups. (C) Effect of TPEN on the increase in cell lethality induced by simultaneous application of zinc pyrithione and H_2O_2. Symbol ($^{\#\#}$) shows significant difference ($P < 0.01$) between a paired groups.

3.2. ZP study

3.2.1. Change in cell lethality by zinc pyrithione

The incubation of cells with 3 μM zinc pyrithione for 120 min did not increase cell lethality. The cell lethality under control condition was 5.6 ± 0.4 % while it was 6.3 ± 0.6 % after incubation with 3 μM zinc pyrithione for 120 min. Therefore, 3 μM zinc pyrithione did not exert cytotoxic action on rat thymocytes under the present experimental conditions. There was also no cytotoxic effect of zinc pyrithione at 1 μM or less.

Micromolar zinc concentrations are cytotoxic to rat thymocytes under oxidative stress conditions induced by H_2O_2 (Matsui et al., 2009a). To see if zinc pyrithione induced similar cytotoxic actions, the time- and concentration-dependent effects of zinc pyrithione on cells suffering from oxidative stress induced by 3 mM H_2O_2 were examined. As shown in Fig. 13A, the simultaneous application of 300 nM zinc pyrithione and 3 mM H_2O_2 time-dependently increased the cell lethality. This increase in cell lethality at 120 min after the start of simultaneous application was significantly greater than that induced by 3 mM H_2O_2 alone. Thus, zinc pyrithione may potentiate the cytotoxicity of H_2O_2. Additionally, at concentrations ranging from 10 nM to 1 μM zinc pyrithione demonstrated a concentration dependence and potentiated the cytotoxicity of 3 mM H_2O_2 when examined 120 min after simultaneous application (Fig. 13B). To reveal the contribution of Zn^{2+} to the potentiation of H_2O_2 cytotoxicity by zinc pyrithione, the effect of 10 μM TPEN, a Zn^{2+} chelator, was examined. In the presence of 10 μM TPEN, the cells were incubated with 3 mM H_2O_2 alone or the combination of 3 mM H_2O_2 and 1 μM zinc pyrithione for 120 min. As shown in Fig. 13C, simultaneous application of 10 μM TPEN significantly attenuated the increase in cell lethality induced by H_2O_2 alone (Matsui et al., 2009b) or the combination of H_2O_2 and zinc pyrithione. The results suggest the contribution of Zn^{2+}.

Figure 13

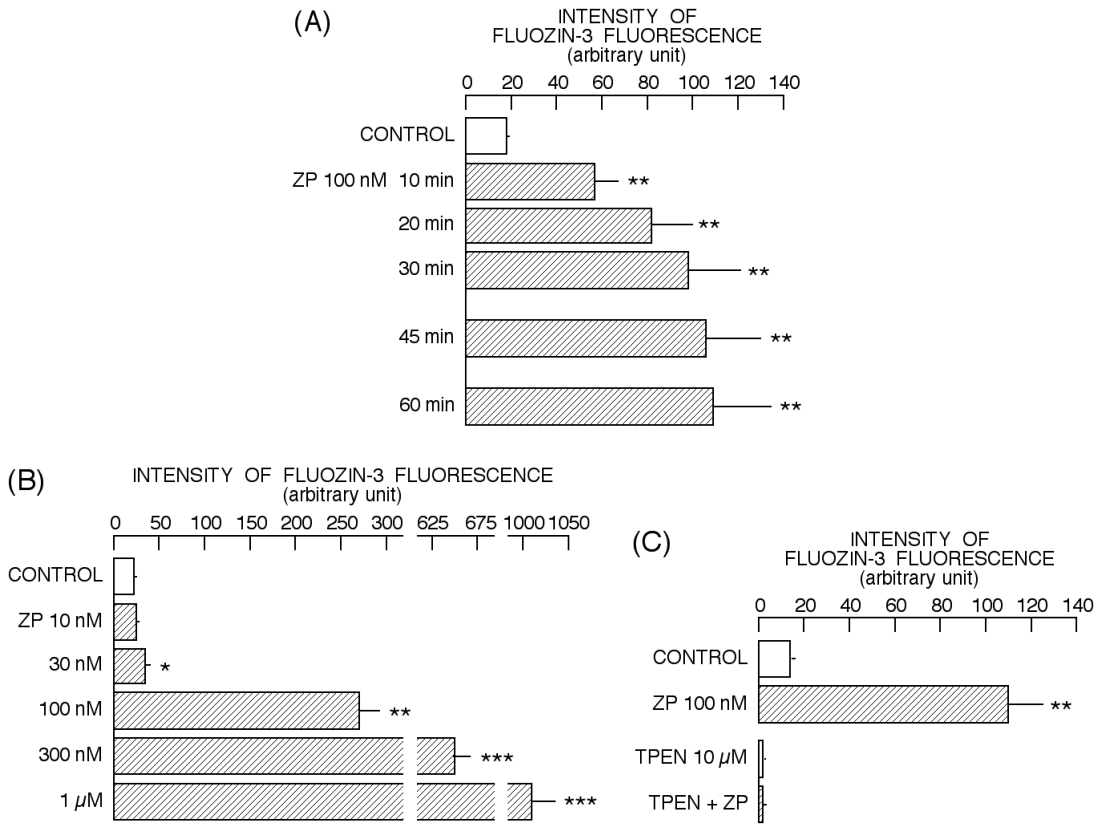

Fig. 13. Change in intracellular Zn^{2+} concentrations by zinc pyrithione. Columns and bars respectively indicate mean and standard deviation of 4 experiments. Symbols (*, **) show significant differences ($P < 0.05$, $P < 0.01$) between control group and respective test groups. (A) Time-dependent change in the intensity of FluoZin-3 fluorescence after the start of zinc pyrithione (ZP) application. (B) Dose-dependent change in the intensity of FluoZin-3 fluorescence by zinc pyrithione. Effects were examined 1 h after the start of application. Large differences (***) masked statistical differences between the control group and the groups of cells treated with 30–100 nM zinc pyrithione; therefore, statistical analysis was conducted on the groups of cells treated with 10–100 nM zinc pyrithione. (C) Effect of TPEN on the augmentation of FluoZin-3 fluorescence by zinc pyrithione.

3.2.2. Change in intracellular Zn^{2+} level by zinc pyrithione

Fig. 13C shows that zinc pyrithione might increase cell susceptibility to oxidative stress induced by H_2O_2 in a zinc-dependent manner. Therefore, the change in intracellular Zn^{2+} level by zinc pyrithione was examined using FluoZin-3, a fluorescent probe for intracellular Zn^{2+} (Gee et al., 2002). As shown in Fig. 14A, zinc pyrithione at 100 nM time-dependently increased the intensity of FluoZin-3 fluorescence after the start of application. The action of 100 nM zinc pyrithione attained a steady-state level within 60 min after application. A concentration-dependent increase in the intensity of FluoZin-3 fluorescence by zinc pyrithione at concentrations ranging from 10 nM to 1 μM was also observed when the effect of zinc pyrithione was examined at 60 min after the application (Fig. 14B). The action of 100 nM zinc pyrithione on FluoZin-3 fluorescence was completely abolished by the simultaneous application of 10 μM TPEN (Fig. 14C).

Figure 14

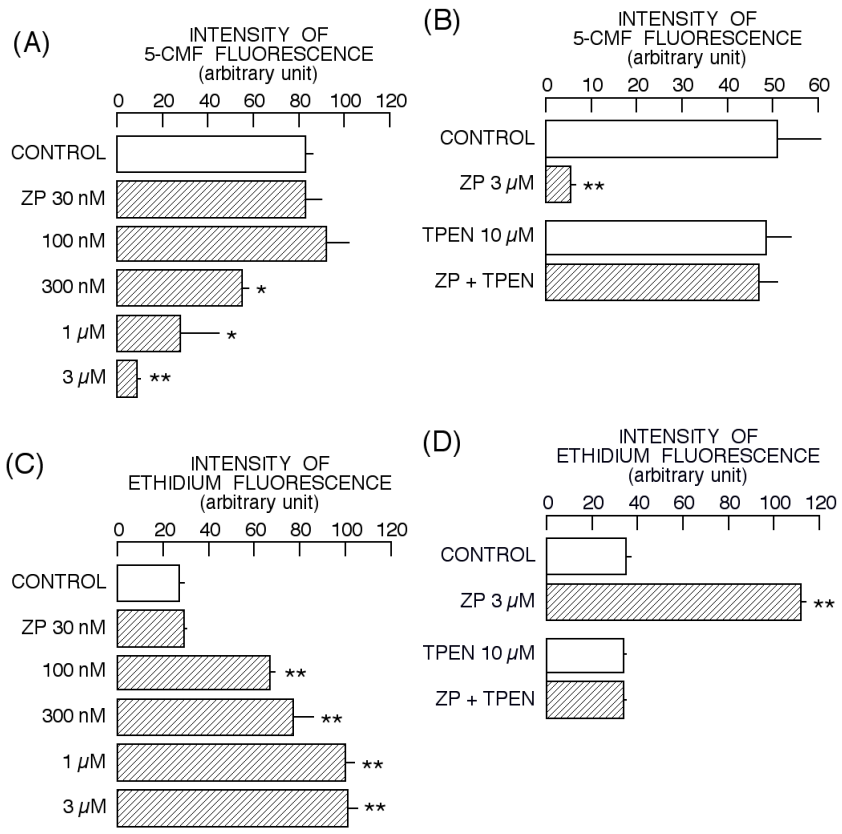

Fig. 14. Changes in cellular contents of nonprotein thiols and superoxide anions by zinc pyrithione. Columns and bars respectively indicate mean and standard deviation of 4 experiments. Symbols (*, **) show significant differences ($P < 0.05$, $P < 0.01$) between control group and respective test groups. (A) Dose-dependent changes in the intensity of 5-CMF fluorescence by zinc pyrithione (ZP). Effects were examined 1 h after the start of application. (B) Effect of TPEN on the change in 5-CMF fluorescence induced by zinc pyrithione. (C) Concentration-dependent change in the fluorescence of cells incubated with dihydroethidium by zinc pyrithione. Effects were examined 1 h after the start of application. (D) Effect of TPEN on the change in fluorescence of cells incubated with dihydroethidium by zinc pyrithione.

3.2.3. Change in cellular content of nonprotein thiols by zinc pyrithione

As shown in Fig. 14, zinc pyrithione, at submicromolar concentrations, time- and concentration-dependently increased intracellular Zn^{2+} level in rat thymocytes. Zinc has been

reported to ameliorate and/or aggravate oxidative stress as described in the introduction. To see if zinc pyrithione affects the cellular content of nonprotein thiols, which help protect against oxidative stress, the effect of zinc pyrithione on cellular thiol content was examined by the use of 5-CMF-DA (Chikahisa et al., 1996). 5-CMF fluorescence was monitored in cells 60 min after the start of zinc pyrithione application. As shown in Fig. 15A, zinc pyrithione at concentrations ranging from 300 nM to 3 μM decreased the intensity of 5-CMF fluorescence in a concentration-dependent manner. TPEN at 10 μM almost completely suppressed the decrease in the intensity of 5-CMF fluorescence by 3 μM zinc pyrithione (Fig. 15B).

(Figure 15 near here)

Figure 15

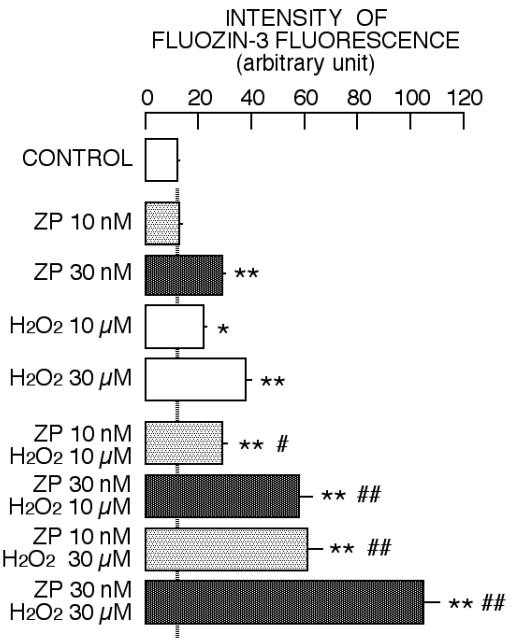

Fig. 15. Change in the intracellular Zn^{2+} concentration by the combination of zinc pyrithione and H_2O_2. Effects were examined 1 h after the start of application of zinc pyrithione (ZP) and H_2O_2. Columns and bars respectively indicate mean and standard deviation of 4 experiments. Symbols (*, **) show significant differences ($P < 0.05$, $P < 0.01$) between control group and respective test groups. Symbols ($^{\#}$, $^{\#\#}$) indicate significant differences ($P < 0.05$, $P < 0.01$) between the group of cells treated only with ZP or H_2O_2 and respective test groups of cells simultaneously treated with ZP and H_2O_2.

3.2.4. Change in cellular content of superoxide anions by zinc pyrithione

Fig. 15A shows that zinc pyrithione at 300 nM or more significantly decreases the cellular content of nonprotein thiols. In order to see if zinc pyrithione increases the cellular content of superoxide anions, which are reactive oxygen species, the fluorescence was monitored 60 min after zinc pyrithione application in cells incubated with dihydroethidium, which is oxidized by superoxide anions to fluorescent ethidium (Fink et al., 2004). As shown in Fig. 15C, zinc pyrithione, at concentrations ranging from 30 nM to 3 μM, increased the intensity of ethidium fluorescence in a concentration-dependent manner, suggesting the increase in cellular content of superoxide anions by zinc pyrithione. The increase by 3 μM zinc pyrithione was completely blocked by 10 μM TPEN (Fig. 15D).

3.2.5. Combination of zinc pyrithione and H_2O_2 at low concentrations

Incubation of rat thymocytes with micromolar H_2O_2 concentrations increases intracellular Zn^{2+} level (Matsui et al., 2009a) and decreases cellular content of glutathione (Chikahisa et al., 1996). Therefore, the simultaneous application of zinc pyrithione and H_2O_2 at low concentrations was expected to synergistically increase intracellular Zn^{2+} concentrations. As shown in Fig. 16, the combinations of 10–30 nM zinc pyrithione and 10–30 μM H_2O_2 greatly augmented FluoZin-3 fluorescence. The increase in intensity of FluoZin-3 fluorescence by the combination was much greater than that observed in the individual applications (Fig. 15). Therefore, zinc pyrithione may greatly increase the susceptibility of cells to oxidative stress.

3.3. CQ study

3.3.1. Clioquinol-induced changes in FluoZin-3 fluorescence

As shown in Fig. 16A, the application of 300 nM clioquinol shifted the histogram of FluoZin-3 fluorescence to a higher intensity, suggesting an increase in the intracellular Zn^{2+} concentration as a result of clioquinol treatment. This augmentation of FluoZin-3 fluorescence by 300 nM clioquinol occurred immediately after clioquinol application and the fluorescence attained its steady state level within 10–30 min. Fig. 16B shows a concentration-dependent augmentation of FluoZin-3 fluorescence when the cells were incubated with clioquinol for 30 min. Clioquinol started to augment the fluorescence at a concentration of 10–30 nM. Increases in the clioquinol concentration (to 100–300 nM) further augmented FluoZin-3 fluorescence. However, when the concentration was increased to 1 μM, clioquinol did not further augment the fluorescence (Fig. 16B). The intensity of FluoZin-3 fluorescence augmented by 1 μM clioquinol was slightly less than that augmented by 300 nM clioquinol.

TPEN completely abolished the clioquinol-induced augmentation of FluoZin-3 fluorescence, suggesting the effect was dependent on Zn^{2+}.

3.3.2. Effects of DTPA and extracellular Zn^{2+} on the clioquinol-induced change in FluoZin-3 fluorescence

To determine whether the clioquinol-induced increase in the intracellular Zn^{2+} concentration was dependent on extracellular Zn^{2+}, the effect of clioquinol on FluoZin-3 fluorescence was examined in the presence of DTPA and $ZnCl_2$. The application of 10 μM DTPA into the suspension slightly decreased the intensity of FluoZin-3 fluorescence. In the presence of DTPA, 100 nM clioquinol completely failed to augment the fluorescence of FluoZin-3 (Fig. 17). The application of 1 μM $ZnCl_2$ into the cell suspension increased the control level of FluoZin-3 fluorescence. Clioquinol at 100 nM further augmented the fluorescence in the presence of $ZnCl_2$. The augmentation by clioquinol in the presence of 1 μM $ZnCl_2$ was much greater than that observed under the control condition (Fig. 17). As shown in Fig. 17, the augmentation of FluoZin-3 fluorescence by clioquinol seemed to be dependent on extracellular Zn^{2+}.

Figure 16

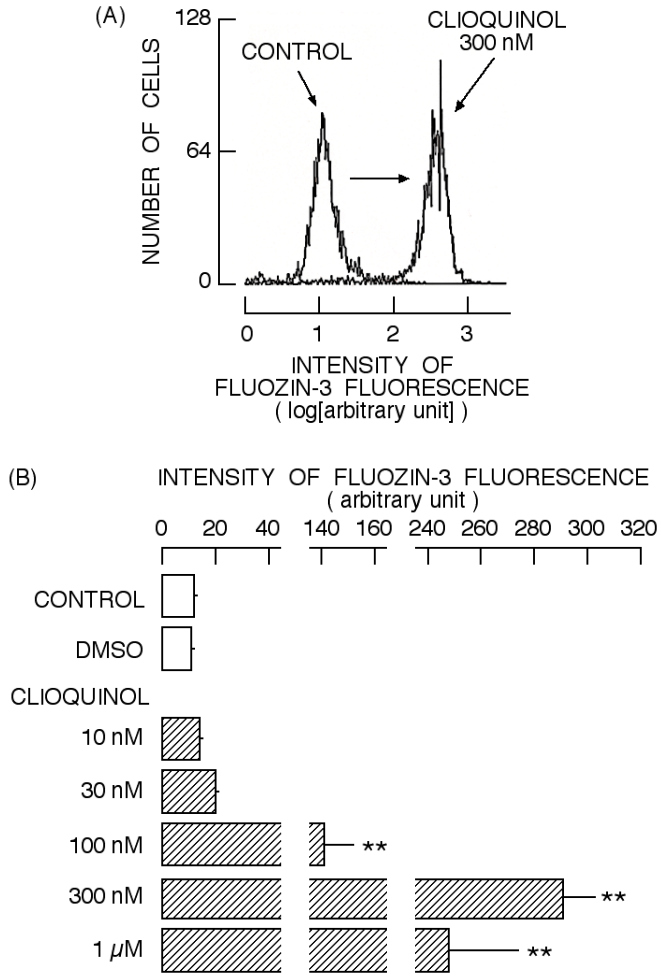

Fig. 16. Clioquinol-induced augmentation of FluoZin-3 fluorescence. (A) A shift in the histogram of FluoZin-3 fluorescence following clioquinol treatment. Each histogram consisted of 2000 cells. The effect of clioquinol was examined 30 min after the start of drug application. (B) The concentration-dependent change in the intensity of FluoZin-3 fluorescence as a result of clioquinol application. Effects were examined 30 min after the start of drug application. The columns and bars indicate the mean and standard deviation, respectively, of 4 experiments. ** indicates a significant difference ($P < 0.01$) between the control groups (CONTROL and DMSO) and the groups of cells treated with clioquinol. It was noted that the intensity of FluoZin-3 fluorescence emitted by the cells treated with 1 μM clioquinol was significantly ($P < 0.05$) lower than that from the cells treated with 300 nM clioquinol.

Figure 17

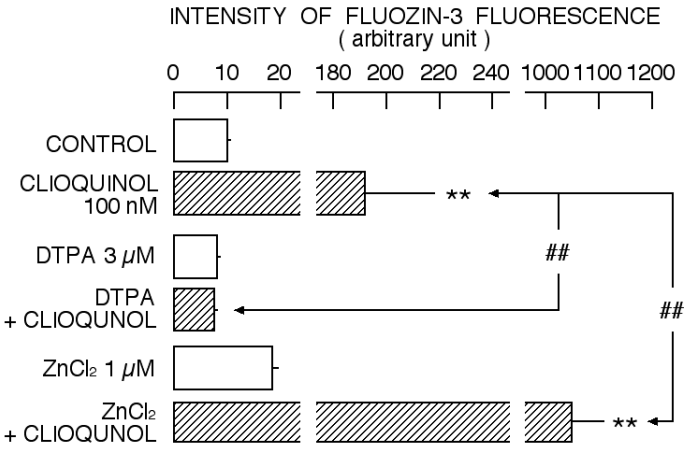

Fig. 17. Changes in the clioquinol-induced augmentation of FluoZin-3 fluorescence as a result of simultaneous application with DTPA or $ZnCl_2$. Effects were examined 30 min after the start of drug application. The columns and bars indicate the mean and standard deviation, respectively, of 4 experiments. ** and ## indicate significant differences ($P < 0.01$) between the groups of cells treated with clioquinol and their control groups, respectively. The experiments were performed in duplicate and reproduced three times. One representative experiment is shown.

3.3.3. Clioquinol-induced changes in Fluo-3 fluorescence

The cell suspension contained 2 mM $CaCl_2$ as a composition of Tyrode's solution and 200–230 nM zinc derived from the cell preparation (Sakanashi et al., 2009). One may argue that clioquinol could also increase the membrane transport of Ca^{2+}, resulting in an increase in intracellular Ca^{2+}. We examined the effect of clioquinol on Fluo-3 fluorescence, an indicator of intracellular Ca^{2+}. As shown in Fig. 18A, clioquinol, at concentrations ranging from 10 to 300 nM, increased the intensity of Fluo-3 fluorescence in a concentration-dependent manner. However, 1 μM clioquinol did not further increase the intensity of Fluo-3 fluorescence. In the presence of 10 μM DTPA, 300 nM clioquinol completely failed to augment Fluo-3 fluorescence (Fig. 18B). Further application of 100 nM A23187 greatly increased the intensity of Fluo-3 fluorescence. Thus, the effect of clioquinol on Fluo-3 fluorescence appeared to be dependent on Zn^{2+}.

Figure 18

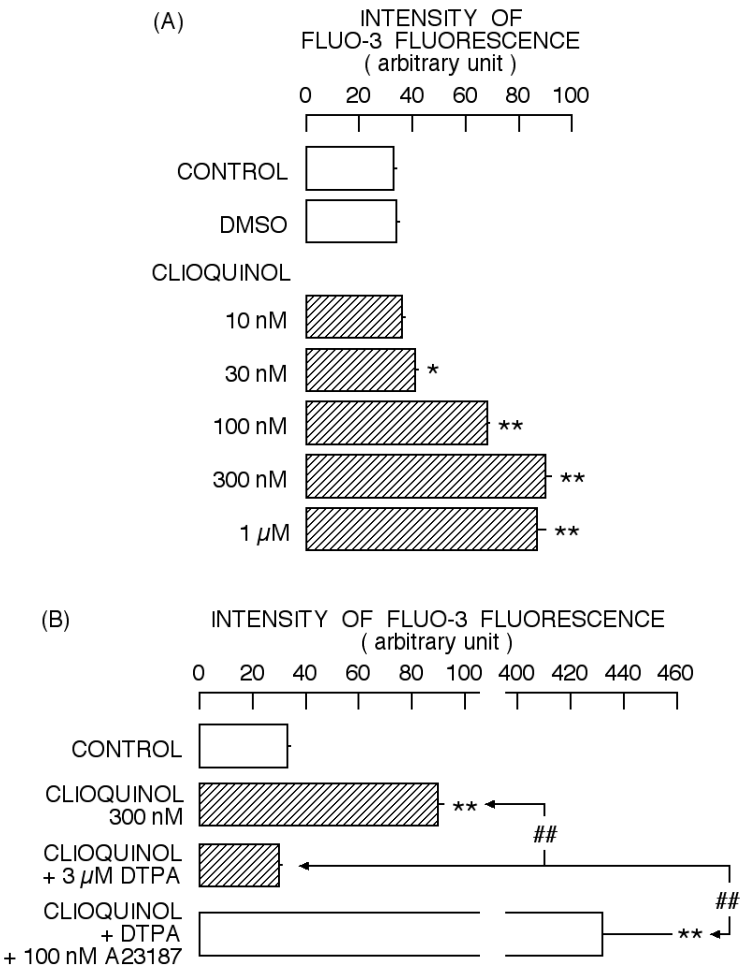

Fig. 18. Augmentation of Fluo-3 fluorescence by clioquinol. (A) The concentration-dependent change in the intensity of Fluo-3 fluorescence induced by clioquinol. Effects were examined 30 min after the start of drug application. The columns and bars indicate the mean and standard deviation, respectively, of 4 experiments. * and ** indicate significant differences ($P < 0.05$ and < 0.01, respectively) between the control groups (CONTROL and DMSO) and the groups of cells treated with clioquinol, respectively. (B) The change in the clioquinol-induced augmentation of Fluo-3 fluorescence as a result of simultaneous application with DTPA. Effects were examined 30 min after the start of drug application. The columns and bars indicate the mean and standard deviation, respectively, of 4 experiments. ** and ## indicate significant differences ($P < 0.01$) between the groups of cells treated with clioquinol and their control groups, respectively.

3.3.4. Effect of clioquinol on FluoZin-3 fluorescence in the presence of DTPA

Clioquinol is believed to be a membrane-permeable chelator of Zn^{2+} and Cu^{2+}. If this is true, membrane-permeable clioquinol would chelate intracellular Zn^{2+} under extracellular Zn^{2+}-free conditions, resulting in a decrease in the intracellular Zn^{2+} concentration. Therefore, the effect of clioquinol on FluoZin-3 fluorescence was examined in the presence of 3 μM DTPA. As shown in Fig. 19, the incubation with clioquinol at concentrations ranging from 300 nM to 10 μM for 60 min attenuated the fluorescence of FluoZin-3 in a concentration-dependent manner.

Figure 19

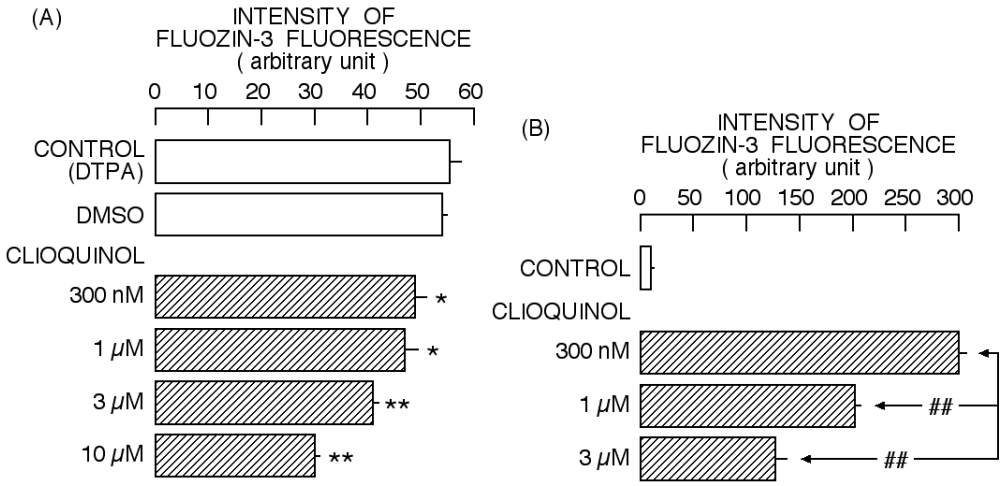

Fig. 19. Effect of clioquinol on FluoZin-3 fluorescence in the presence of DTPA. (A) The concentration-dependent change in the intensity of FluoZin-3 fluorescence as a result of clioquinol treatment. Effects were examined 30 min after the start of drug application. The columns and bars indicate the mean and standard deviation, respectively, of 4 experiments. * and ** indicate significant differences ($P < 0.05$ and < 0.01, respectively) between the control groups (CONTROL and DMSO) and the groups of cells treated with clioquinol, respectively. (B) The effect of micromolar concentrations of clioquinol on FluoZin-3 fluorescence in the absence of DTPA. Effects were examined 30 min after the start of drug application. The columns and bars indicate the mean and standard deviation, respectively, of 3 experiments. ## indicates significant differences ($P < 0.01$) between the groups of cells treated with clioquinol. The experiments were performed in duplicate and reproduced three times. One representative experiment is shown.

3.3.5. Clioquinol-induced changes in cell death under oxidative stress induced by H_2O_2

The propidium iodide fluorescence of rat thymocytes treated with 300 μM H_2O_2 alone, 100 nM clioquinol, or a combination of both after incubation for 4 h is shown in Fig. 20A. The proportion of cells exhibiting propidium fluorescence (i.e., dead cells) after 4 h incubation with a combination of 100 nM clioquinol and 300 μM H_2O_2 was significantly greater than that of cells treated with either 300 μM H_2O_2 or 100 nM clioquinol alone. Thus, clioquinol at a concentration of 100 nM increased the cytotoxicity of H_2O_2. Fig. 20A also shows results obtained from cells treated with 300 μM H_2O_2 alone, 1 μM clioquinol alone, and a combination of both. The proportion of cells exhibiting propidium fluorescence after 4 h incubation with a combination of 1 μM clioquinol and 300 μM H_2O_2 was significantly less than that of cells treated with 300 μM H_2O_2 alone. Thus, clioquinol at a concentration of 1 μM attenuated the cytotoxicity of H_2O_2.

The concentration-dependent changes in the cytotoxicity of 300 μM H_2O_2 induced by clioquinol showed a bell-shaped curve (Fig. 20B). H_2O_2 cytotoxicity was the highest at a concentration of 100 nM clioquinol. We observed that clioquinol at a concentration of 100 nM but not 30 nM increased the cytotoxicity of H_2O_2 within a concentration range of 100–300 μM (Fig. 20C). Further, incubation with 30–300 nM clioquinol alone for 4 h did not change the lethality in rat thymocytes.

Figure 20

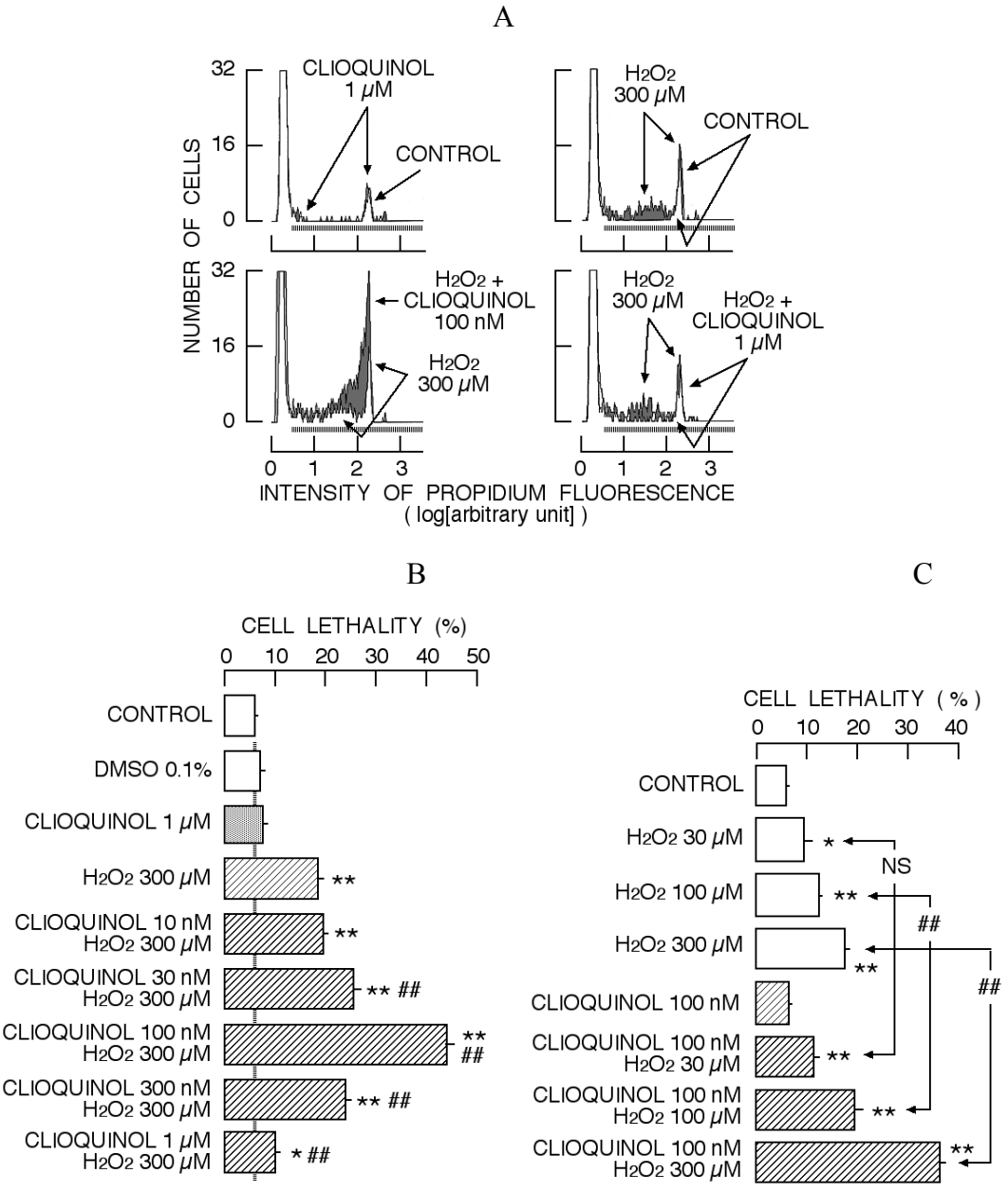

Fig. 20. Clioquinol-induced changes in oxidative stress-induced cell death. (A) Histogram of propidium fluorescence in rat thymocytes treated with clioquinol, hydrogen peroxide (H_2O_2), or a combination of both. Left upper panel, control (open) and 1 μM clioquinol (filled); right upper panel, control (open) and 300 μM H_2O_2 (filled); left lower panel, 300 μM H_2O_2 without (open) and with (filled) 100 nM clioquinol; and right lower panel, 300 μM H_2O_2 without (filled) and with (open) 1 μM clioquinol. Data in each histogram were derived from 2000 cells. (B)

Clioquinol-induced changes in cell death (percentage) under conditions of oxidative stress induced by 300 μM H_2O_2. Columns and bars indicate the means and standard deviations of 4 experiments. Asterisks indicate significant differences in cell death (*P < 0.05, **P < 0.01) between control groups (CONTROL and DMSO, 0.1%). $^{\#}$ denotes significant differences in cell death between cells treated with H_2O_2 alone and cells simultaneously treated with H_2O_2 and clioquinol. (C) Effect of 100 nM clioquinol on cells treated with 30–300 μM H_2O_2. Asterisks indicate significant differences (*P < 0.05, **P < 0.01) between the control cells (CONTROL) and those treated with H_2O_2 alone, clioquinol alone, or a combination of both. $^{\#}$ denotes significant differences ($^{\#\#}$ P < 0.01) between paired groups, as indicated by arrows. NS, no significant difference.

3.3.6. Effects of Zn^{2+} chelators on clioquinol-induced increases in cell death under oxidative stress

We examined the effects of the Zn^{2+} chelators DTPA and TPEN on increases in cell death induced by the simultaneous application of 100 nM clioquinol and 300 μM H_2O_2 to determine whether Zn^{2+} is involved in the cell death. TPEN (10 μM), an intracellular Zn^{2+} chelator, completely suppressed the H_2O_2 (300 μM)-induced increase in the number of cells showing propidium fluorescence, while DTPA (10 μM), an extracellular Zn^{2+} chelator, had no effect on the number of cells showing propidium fluorescence (Fig. 21). The increase in the number of cells showing propidium fluorescence after simultaneous treatment with 100 nM clioquinol and 300 μM H_2O_2 significantly decreased after treatment with 10 μM TPEN and 10 μM DTPA, and TPEN completely suppressed the above effect. TPEN at concentrations of 300 nM or more decreased the H_2O_2-induced increase in cell lethality in a concentration-dependent manner.

Figure 21

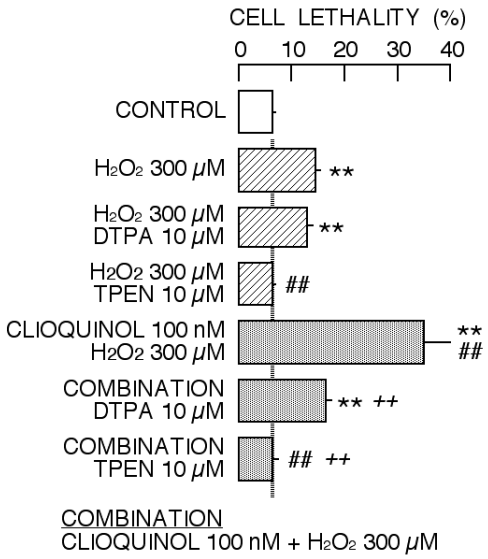

Fig. 21. Effects of Zn^{2+} chelators on cells treated with hydrogen peroxide (H_2O_2) alone or a combination of H_2O_2 and clioquinol. Asterisks indicate significant differences in cell death (**, $P < 0.01$) between control cells (CONTROL) and drug(s)-treated cells. Symbol (##) indicates significant differences (##, $P < 0.01$) between cells treated with H_2O_2 alone and other groups of drug(s)-treated cells. Symbol (++) indicates significant differences (++, $P < 0.01$) between cells simultaneously treated with H_2O_2 and clioquinol and those additionally treated with a Zn^{2+} chelator.

3.3.7. Effects of clioquinol on cell death induced by H_2O_2 in the presence of DTPA

An initial incubation with H_2O_2 increased the number of annexin V-positive live cells, which was followed by an increase in cell death (Oyama et al., 1999). Treatment with a combination of 100 nM clioquinol and 300 μM H_2O_2 increased the transition of the cells from intact living cells to annexin V-positive live cells and subsequently to dead cells. However, 10 μM DTPA significantly inhibited the increase in cell death induced by 100 nM clioquinol (Fig. 22).

Figure 22

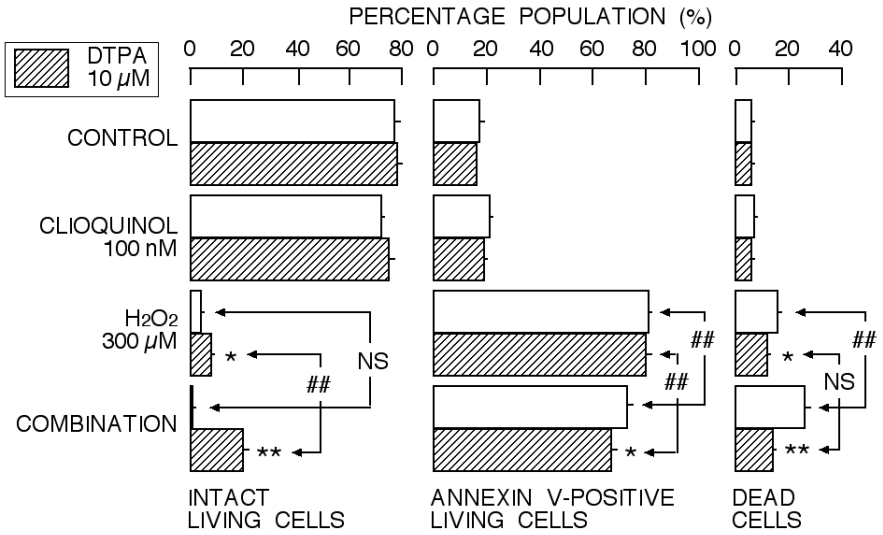

Fig. 22. Changes in cell populations after incubation with clioquinol alone, H_2O_2 alone, or a combination of both. Columns and bars show means and standard deviations of 4 samples. Asterisks show significant differences (*, $P < 0.05$ and **, $P < 0.01$) between the groups with and without diethylenetriamine-N,N,N',N'',N''-pentaacetic acid (DTPA) treatment. Symbol (##) indicates significant differences (##, $P < 0.01$) between paired groups, as indicated with arrows. NS, no significant difference.

3.3.8. Clioquinol-induced changes in intracellular Zn^{2+} levels without and with oxidative stress

The increase in FluoZin-3 fluorescence by clioquinol at concentrations ranging from 10 nM to 3 μM showed a bell-shaped curve (Fig. 23A). Clioquinol at concentrations of 100 nM or more significantly increased the intensity of FluoZin-3 fluorescence. However, 1–3 μM clioquinol showed a significantly lesser increase in FluoZin-3 fluorescence than 300 nM clioquinol did. In addition, clioquinol at concentrations ranging from 30 nM to 3 μM significantly increased the intensity of FluoZin-3 fluorescence induced by 300 μM H_2O_2 (Fig. 23B). This concentration-dependent effect of clioquinol also followed a bell-shaped curve although the combination of clioquinol and H_2O_2 had a synergistic effect on the increase in FluoZin-3 fluorescence.

Figure 23

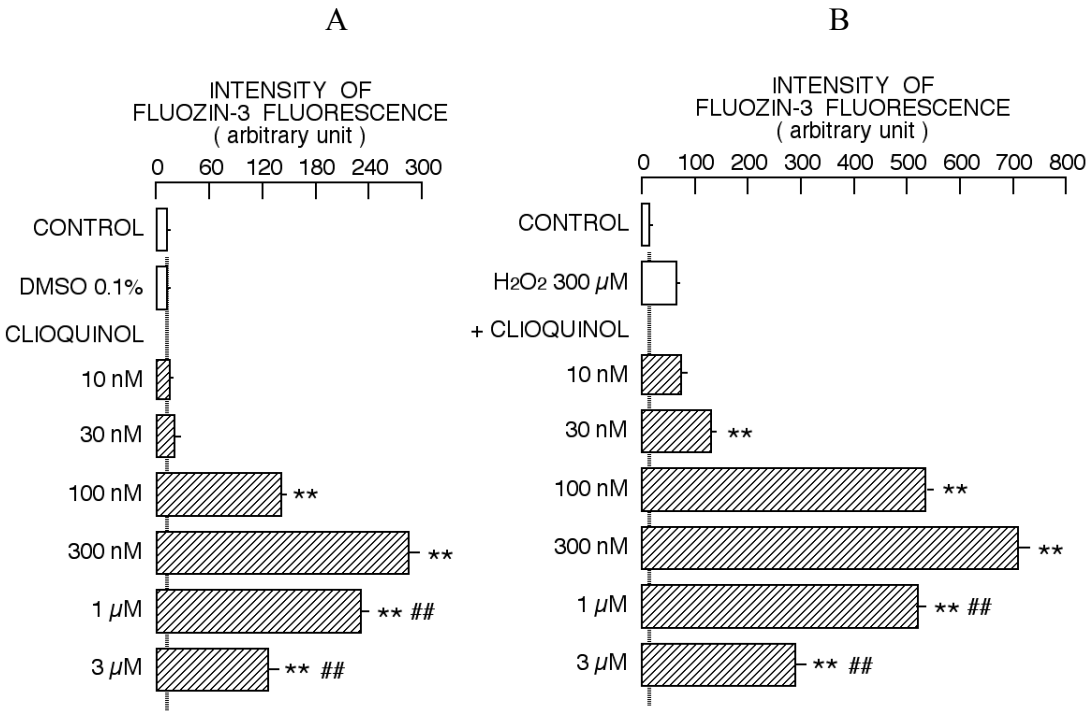

Fig. 23. Clioquinol-induced changes in intracellular Zn^{2+} concentration in cells treated without (A) and with (B) hydrogen peroxide (H_2O_2). Columns and bars show mean FluoZin-3 fluorescence intensities and standard deviations of 4 samples. Asterisks denote significant differences (**, $P < 0.01$) between control groups (A: CONTROL and DMSO, 0.1%, B: H_2O_2, 300 μM) and those treated with clioquinol. Symbol (##) indicates significant reductions in peak responses elicited by 300 nM clioquinol (**, $P < 0.01$).

3.3.9. Clioquinol-induced changes in intracellular Zn^{2+} levels in presence and absence of extracellular Zn^{2+}

When 1 μM $ZnCl_2$ was added to the cell suspension, FluoZin-3 fluorescence significantly increased in the control cells (Kinazaki et al., 2011), and this effect was further enhanced by 10 nM clioquinol. However, the bell-shaped concentration-response relationship of clioquinol was less apparent in the range of 100 nM to 3 μM (Fig. 24A). In the presence of 10 μM DTPA, clioquinol at concentrations of 300 nM or more (up to 3 μM) decreased FluoZin-3 fluorescence in a concentration-dependent manner (Fig. 24B). The bell-shaped concentration-response relationship of clioquinol-induced responses was no longer apparent.

Figure 24

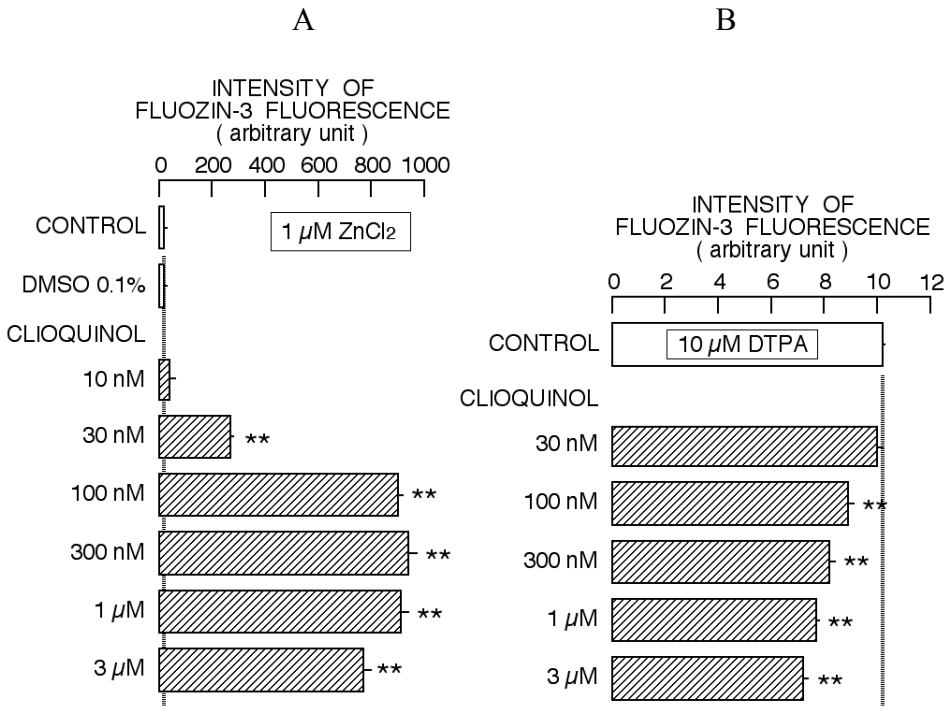

Fig. 24. Clioquinol-induced changes in intracellular Zn^{2+} concentrations in cells treated with 1 μM zinc chloride ($ZnCl_2$) (A) or 10 μM diethylenetriamine- N,N,N',N'',N''-pentaacetic acid (DTPA) (B). Columns and bars show mean FluoZin-3 fluorescence intensities and standard deviations of 4 samples. Asterisks denote significant differences (**, $P < 0.01$) between the control groups (A: CONTROL and DMSO, 0.1%, B: CONTROL) and those treated with clioquinol.

3.3.10. Clioquinol-induced changes in cellular oxidant levels

CM-DCF fluorescence is a marker of cellular oxidant levels (Koopman et al., 2007). Incubation of cells with clioquinol at concentrations ranging from 100 nM to 3 μM for 3–4 h significantly decreased the intensity of CM-DCF fluorescence, which indicated that incubation with clioquinol at concentrations of 100 nM or more (up to 3 μM) decreased cellular oxidant levels (Fig. 25).

Figure 25

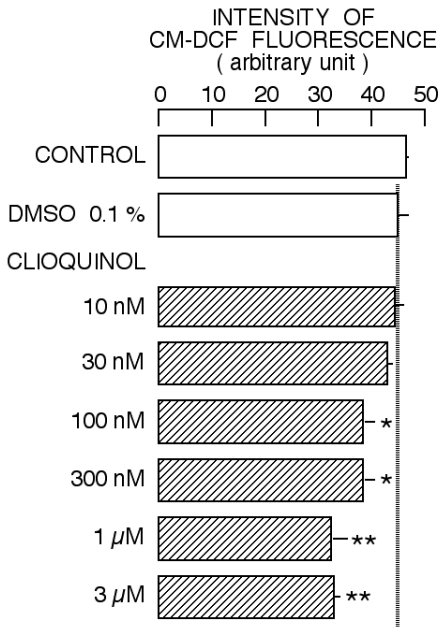

Fig. 25. Clioquinol-induced decreases in cellular oxidant levels. Columns and bars show mean CM-DCF fluorescence intensities and standard deviations of 4 samples. Asterisks indicate significant differences (*, $P < 0.05$ and **, $P < 0.01$) between control cells (DMSO, 0.1%) and those treated with clioquinol.

4.Discussion

4.1. PS80 study

4.1.1. Academic implication

Polysorbate 80 is a non-ionic surfactant used widely in pharmaceutical products, cosmetics, and foods because of its effectiveness at low concentrations and relative low toxicity (National Toxicology Program, 1992). This surfactant is employed in the formula of water-insoluble anticancer agents such as docetaxel and etoposide for intravenous application. Furthermore, colloidal carries (nanoparticles) coated with polysorbate 80 enhanced transport of doxorubicin into the brain (Gulyaev et al., 1999; Gelperina et al., 2002). The delivery of nanoparticle drugs requires polysorbate 80 as a solvent (Chakraborty et al., 2009; Gabathuler, 2010; Kumari et al., 2010). Thus, polysorbate 80 possesses important implications for cancer chemotherapy (Loos et al., 2003; ten Tije et al., 2003; Engels et al., 2007).

Under in vitro experimental conditions, polysorbate 80 was found to bind physiologically-important ions such as Na^+, K^+, and Ca^{2+} and transport them through a model membrane (Thoman, 1999). It also affected membrane and mitochondrial functions (Oberle et al., 1995; Tsujino et al., 1999; Rege et al., 2002). Furthermore, polysorbate 80 at plasma concentrations decreased cellular thiol content that induced susceptibility to oxidative stress (Hirama et al., 2004; Tatsuishi et al., 2005). In our recent studies, the chemicals decreasing cellular thiol content increased intracellular Zn^{2+} concentration by intracellular Zn^{2+} release (Hashimoto et al., 2009; Oyama et al., 2009; Kawanai et al., 2009). Thus, polysorbate 80 may increase intracellular Zn^{2+} concentration. Zn^{2+} is the second most prevalent trace element and it is involved in the structure and function of over 300 enzymes (Prasad, 1995). Zn^{2+} stimulates the activity of approximately 100 enzymes (Sandstead, 1994). Therefore, an abnormal increase in intracellular Zn^{2+} concentration by polysorbate 80 may cause cytotoxic phenomena. In this study, therefore, we have cytometrically examined the effect of polysorbate 80 on FluoZin-3 fluorescence, an indicator for intracellular Zn^{2+}, and the influence of $ZnCl_2$ on the cytotoxicity of polysorbate 80 in rat thymocytes in order to test the possibilities described above.

4.1.2. Elevation of intracellular Zn^{2+} concentration by polysorbate 80

Zn^{2+} is complexed to intracellular thiol such as metallothionein and glutathione (Diaz-Cruz et al., 1998; Jacob et al., 1998; Maret and Vallee, 1998; Gelinsky et al., 2003). Modification from intracellular thiol (sulfhydryl group) to disulfide releases Zn^{2+} (Maret, 1994; Quesada et al., 1996; Jiang et al., 1998). Polysorbate 80 at concentrations ranging from 10 μg/ml to 300 μg/ml decreases the intensity of 5-CMF fluorescence, a fluorescent indicator for cellular thiol content, in a concentration-dependent manner (Hirama et al., 2004). The result of Fig. 2 in this study was compared with that of Hirama et al. (2004) to see if there is a relation between the changes in FluoZin-3 and 5-CMF fluorescence by polysorbate 80 at concentrations ranging from 1 μg/ml to 300 μg/ml. The correlation coefficient was -0.978 (Fig. 11). The relation presumably suggests that the decrease in cellular thiol content by polysorbate 80 induces the increase in intracellular Zn^{2+} concentration. In addition, it is likely that polysorbate 80 increases membrane Zn^{2+} permeability because of following observations. As shown in Fig. 3, the addition of 30 μM $ZnCl_2$ to the cell suspension increased the base intensity of FluoZin-3 fluorescence and 30 μg/ml polysorbate 80 further increased the intensity in the presence of $ZnCl_2$. The degree of the augmentation of FluoZin-3 fluorescence by the combination of polysorbate 80 and $ZnCl_2$ was much greater than that by polysorbate 80 alone

(Fig. 3).

4.1.3. Cytotoxicity of the combination of polysorbate 80 and $ZnCl_2$

The simultaneous application of $ZnCl_2$ and polysorbate 80 significantly increased the population of dead cells (Figs. 4 and 5). The simultaneous application of 10 μM $ZnCl_2$ and 10 mM hydrogen peroxide greatly increased the population of dead cells (Matsui et al., 2009). It is likely that polysorbate 80 at 30 μg/ml induces oxidative stress because of following reasons. Polysorbate 80 decreased the intensity of 5-CMF fluorescence (Hirama et al., 2004) and increased the intensities of fluorescence's monitored from cells incubated with dihydroethidium and DCFH-DA, respectively (Fig. 9), suggesting the decrease in cellular thiol content and the increases in reactive oxygen species. Thus, $ZnCl_2$ may potentiate the cytotoxicity of reactive oxygen species. However, it is difficult to conclude the mechanism because of following reasons. Although zinc itself increased cellular glutathione content (Fig. 9A), zinc did not attenuate the cytotoxicity of polysorbate 80. An excess increase in intracellular Zn^{2+} concentration in the presence of polysorbate 80 may induce zinc-dependent cytotoxicity that is not related to cellular redox state. Furthermore, curcumin, an antioxidant against hydrogen peroxide, did not affect the cytotoxicity induced by the combination of polysorbate 80 and $ZnCl_2$ (Fig. 10).

The cell death by the simultaneous application was associated with cell shrinkage (Fig. 6) and phosphatidylserine externalization (Figs. 7 and 8), characteristics during an early stage of apoptosis (Klassen et al., 1993; Koopman et al., 1994; Beauvais et al., 1995; Vermes et al., 1995). However, the combination of polysorbate 80 and $ZnCl_2$ did not increase the population of cells with hypodiploid DNA, a marker of apoptosis. Therefore, the type of cell death induced by the combination is likely necrosis with some apoptotic characteristics. The increase in intracellular Zn^{2+} concentration by the combination may attenuate the process of apoptosis because DNA fragmentation is inhibited by Zn^{2+} (Zalewski et al., 1991; Barbieri et al., 1992; Sunderman, 1995).

4.1.4. Toxicological implications

Maximum plasma concentration of polysorbate 80 in cancer patients receiving docetaxel was greater than 100 μg/ml (Baker et al., 2004). The median end-infusion plasma concentration of polysorbate 80 in nine patients receiving a 1 h infusion of docetaxel was about 100 μg/ml (Webster et al., 1997). Therefore, the concentrations (1-300 μg/ml) of polysorbate 80 used in this in vitro study were achievable under the in vivo (clinical) condition. In the case of zinc, the mean concentration in human plasma is < 15 μM, which is considerably less than in

many other tissues (Brown, 1998). The total amount of zinc circulating in plasma is < 0.2% of the total body zinc content. The plasma zinc concentration reached 30 μM after prophylactic zinc supplementation (Wuehler et al., 2008). In hyperzincemia, it was greater than 200 μM (Sampson et al., 1997). Thus, the zinc concentrations (10-100 μM) used in this in vitro study were also reasonable. Although there is no report that polysorbate 80 and zinc salt are simultaneously applied to human as far as our knowledge, it is speculated that zinc may provide some benefits in cancer treatment with docetaxel of which the solvent is polysorbate 80 because of following reports. Zinc replenishment reduced the development of tumors (Fong et al., 2001). Zinc accumulation induced apoptosis in human epithelial ovarian cells (Bae et al., 2006) and in choriocarcinoma cells (Bae et al., 2007). Zinc exerted anti-tumor action on colon cancer (Jaiswal and Narayan, 2004) and prostate cancer (Franklin and Costello, 2007).

In conclusion, it is unlikely that polysorbate 80 and zinc (or $ZnCl_2$) are intentionally co-administrated under clinical condition. However, polysorbate 80 is a solvent for some anticancer agents while zinc is used as a nutritional supplement. Therefore, only one possible situation is that the patients receiving intravenous application of drugs containing polysorbate 80 as a solvent take such a supplement. Such patients are recommended to avoid taking zinc supplement.

4.2. ZP study

4.2.1. Academic implication

Zinc pyrithione is an agent possessing antimicrobial activity contained in health care products (Guthery et al., 2005) and is approved for over-the-counter topical use as a treatment for dandruff (Marks et al., 1985; Warner et al., 2001). Consumer products containing zinc pyrithione are disposed of down residential drains. Recently, this agent was introduced as a novel antifouling agent (Konstantinou and Albanis, 2004). Antifouling agents in paints and coatings inhibit the growth of barnacles and other marine organisms on a ship's bottom by their biocidal actions. Previously, the most commonly used antifouling agent was the tributyltin moiety. However, the use of tributyltin was banned worldwide because of its harmful impact on the aquatic ecosystem (Ebdon et al., 1989; Antizar-Ladislao, 2008). Thus, antifouling agents can exert cytotoxic or biocidal actions in nature. In the case of zinc pyrithione, the toxicities were tested in preparations of fish (Goka, 1999), urchins (Bellas et al., 2005), ascidians (Bellas, 2005), plankton (Hjorth et al., 2006), amphipods (Bao et al., 2008), diatoms (Bao et al., 2008), polychaetes (Bao et al., 2008; Marcheselli et al., 2010a), and mussels (Marcheselli et al., 2010b, 2011). This antifouling agent seems to be more persistent than

expected in the coastal environment and to have potential to bioaccumulate (Maraldo and Dahllöf, 2004; Marcheselli et al., 2010b). Therefore, it is necessary to increase the information concerning the toxicity of zinc pyrithione to mammals and mammalian cells if the agent is used as an antifouling agent. As for mammalian cells, the toxicity of zinc pyrithione was examined in kidney cells (Gibson et al., 1985), dermal fibroblasts (Priestley and Brown, 1980; Rudolf and Cervinka, 2011), lymphoma cells (Mann and Fraker, 2005), laryngeal carcinoma cells (Rudolf and Cervinka, 2010), and reconstructed epidermis cells (Lamore and Wondrak, 2011). Zinc pyrithione increases the intracellular Zn^{2+} concentration that is probably responsible for dermal cell cytotoxicity (Rudolf and Cervinka, 2010, 2011; Lamore and Wondrak, 2011). On the contrary, zinc pyrithione salvages reperfusion injury in cardiomyocytes (Kasi et al., 2011). Zinc ameliorates oxidative stress induced by ischemia (Sirmali et al., 2007), indomethacin (Varghese et al., 2009), cadmium (Messaoudi et al., 2009; Banni et al., 2011), arsenic (Kumar et al., 2010), and mercury (Calgaroto et al., 2011). However, zinc itself induces oxidative stress in several types of preparations (Figueiredo-Pereira et al., 1999; Lin et al., 2005; Cabreiro et al., 2009; Morina et al., 2010; Singh et al., 2011). The relationship between zinc and oxidative stress is controversial. It is proposed that, in rat thymocytes, the decrease in cellular content of nonprotein thiols increases the intracellular Zn^{2+} level while the increase in intracellular Zn^{2+} increases the cellular content of nonprotein thiols (Kinazaki et al., 2011). Therefore, zinc pyrithione may exert diverse actions, associated with an increase in intracellular Zn^{2+} concentration.

Previous work has shown the cytotoxic action of micromolar zinc on cells enduring oxidative stress (Matsui et al., 2009a). Therefore, in this study we examined the effect of zinc pyrithione on cells suffering oxidative stress. Additionally, we characterized the mechanism of cytotoxicity associated with zinc pyrithione and cells suffering oxidative stress. This study aimed to reveal new aspects of the toxic action of zinc pyrithione as an antifouling agent.

4.2.2. Effects of zinc pyrithione

Zinc pyrithione at 3 μM or less did not exert cytotoxic action on rat thymocytes when incubated for 120 min. However, nanomolar concentrations of zinc pyrithione potentiate the cytotoxicity of H_2O_2 (Fig. 13A and 13B). Zinc pyrithione increased the intensity of FluoZin-3 fluorescence (Fig. 14A and 14B), decreased the intensity of 5-CMF fluorescence (Fig. 15A), and increased the intensity of fluorescence in cells incubated with dihydroethidium (Fig. 15B). Such actions of zinc pyrithione were greatly attenuated by TPEN, a Zn^{2+} chelator. The threshold concentration of zinc pyrithione increased depending on the fluorescent probe used:

FluoZin-3 fluorescence for intracellular Zn^{2+} (30 nM, Fig. 14B), ethidium fluorescence for superoxide anions (100 nM, Fig. 15A), and 5-CMF fluorescence for cellular nonprotein thiols (300 nM, Fig. 15C). From Figs. 14 and 15, it is suggested that zinc pyrithione increases intracellular Zn^{2+} concentration, which subsequently induces the generation of superoxide anions, resulting in the decrease in cellular content of nonprotein thiols (mainly glutathione). Zinc induces oxidative stress (Figueiredo-Pereira et al., 1999; Lin et al., 2005; Cabreiro et al., 2009; Morina et al., 2010; Singh et al., 2011) and oxidative stress increases intracellular Zn^{2+} concentration (Cima et al., 2006; Kröncke, 2007; Matsui et al., 2009a). Therefore, there is a possibility of facilitative interactions between oxidative stress and intracellular Zn^{2+}. Externally-applied $ZnCl_2$ alone increases the intensity of 5-CMF fluorescence, an indicator of cellular glutathione, under normal conditions (Kinazaki et al., 2011). This increase in cellular content of glutathione is associated with the increase in intracellular Zn^{2+} level (Kinazaki et al., 2011). Although both $ZnCl_2$ and zinc pyrithione increase intracellular Zn^{2+} concentration, the increase in intracellular Zn^{2+} level by $ZnCl_2$ is completely attenuated by cold conditions (Kimura et al., 2011), but not by zinc pyrithione (Oyama and Oyama, unpublished observation). Zinc pyrithione may facilitate Zn^{2+} transport in membranes of cellular compartments including cellular organelles such as mitochondria, while $ZnCl_2$ does not. It is unlikely that the cellular action of zinc pyrithione is identical to that of $ZnCl_2$.

Zinc pyrithione in water solution make dimer complex that quickly dissociate via scission of one of Zn^{2+} coordinate bond (Barnett et al., 1977). Therefore, physicochemical property of zinc pyrithione may vary depending on chemical structure. Physicochemical property of chemicals is one of factors that affect membrane permeation and cellular accumulation. The mechanism of zinc pyrithione to augment the cytotoxicity of H_2O_2 may be complex. In this aspect, further analysis on interaction between zinc pyrithione and membranes will be necessary to elucidate the action of zinc pyrithione.

4.2.3. Toxicological implications

Highly reactive oxygen species are formed during the normal process of metabolism in biological systems utilizing oxygen (Dickinson and Chang, 2011). Therefore, many cells possess defense mechanisms against oxidative stress (Hayes and McLellan, 1999). Many pathological states (diseases) are associated with oxidative stress and oxidative stress is a major cause of cell death (Giustarini et al., 2009; Pellegrini and Baldari, 2009). Furthermore, several types of metals and chemicals induce oxidative stress (McMillian et al., 2005; Singh et al., 2007; Romieu et al., 2008; Migliore and Coppedè, 2009; Jomova and Valko, 2011). In this

study, zinc pyrithione, a novel antifouling agent, at nanomolar concentrations increased the cell lethality of rat thymocytes exposed to H_2O_2 (Fig. 13). Thus, zinc pyrithione at 10 nM (or greater) seems to increase cell susceptibility to oxidative stress. Cytotoxicity of zinc pyrithione alone on rat thymocytes was not observed when the cells were incubated with 3 μM zinc pyrithione for 3 hr. The threshold concentration of zinc pyrithione required to increase the cell susceptibility to oxidative stress was 10 nM (Fig. 13). Therefore, zinc pyrithione at nanomolar concentrations may exert severe cytotoxic actions on cells in the presence of chemicals that induce oxidative stress. If so, zinc pyrithione leaked from antifouling materials to the surrounding environment would be a risk factor for the aquatic ecosystem. Alternatively, the combination of zinc pyrithione with chemicals inducing oxidative stress may become a potent antifouling ingredient.

Zinc is known to play a central role in the immune system and it is clear that zinc is crucial for normal development and function of cells mediating immunity (Shankar and Prasad, 1998). In this study, zinc pyrithione at sublethal concentrations is suggested to disturb intracellular Zn^{2+} homeostasis in rat thymocytes (Fig. 14). At present we have no evidence for the malfunction of thymocytes linked to excessive increase in intracellular Zn^{2+} level by zinc pyrithione. However, zinc is known to cause inhibition of apoptosis in murine thymocytes (Barbieri et al., 1992; Provinciali et al., 1995; Chukhlovin et al., 2001). The primary function of thymocytes is the maturation of T lymphocytes. The function of T cells, to recognize foreign antigens, is mediated by T cell receptors. Cells that fail to produce a functional receptor are eliminated by apoptosis, and apoptosis is the fate of most thymocytes (Yang and Ashwell, 1999). Decrease in cellular content of glutathione was reported during apoptosis in murine thymocytes (Beaver and Waring, 1995; Macho et al., 1997). Therefore, the excessive increase in intracellular Zn^{2+} concentration and oxidative stress induced by zinc pyrithione may increase the survival of cells that are assumed to be extinct, resulting in a change in the immune competent system.

4.3. CQ study-Part 1 – Clioquinol-induced increase and decrease in the intracellular Zn^{2+} level

4.3.1. Academic implication for CQ study

Chelation therapy is a common therapy for heavy metal intoxication because the administration of hydrophilic chelating agents systemically removes heavy metals from the body. The usefulness of chelation therapy in some neurological diseases (or neurodegenerative disorders) has been proposed (Cai et al., 2005; Gracia and Snodgrass, 2007; Bolognin et al., 2009; Hegde et al., 2009). In the case of brain diseases, chelating agents must

pass across the blood-brain barrier. Such agents are generally lipophilic (or hydrophobic). One may argue the possibility, therefore, that lipophilic agents possessing a chelating property also pass across the membranes, resulting in changes in the intracellular amounts of chelatable ions. In this study, we have tested this possibility.

One important chelating agent is clioquinol, 5-chloro-7-iodo-8-hydroxyquioline. Clioquinol is hydrophobic and selectively binds Zn^{2+} and Cu^{2+} with a greater affinity than that with which it binds Ca^{2+} and Zn^{2+} (Cherny et al., 2001; Raman et al., 2005). Clioquinol can dissolve amyloid deposits because Zn^{2+} and Cu^{2+} are involved in the deposition and stabilization of amyloid plaques (Atwood et al., 2000; Curtain et al., 2001). Clinical trials with clioquinol and Alzheimer disease have been conducted (Ritchie et al., 2003; Lannfelt et al., 2008). Furthermore, clioquinol induces cell death in malignant cells by inhibiting proteasome (Daniel et al., 2005). Thus, clioquinol is emerging as a potential therapy for Alzheimer's disease and cancer. However, while clioquinol increased the intracellular Zn^{2+} concentration in some cell preparations (Anderson et al., 2009; Park et al., 2011), it attenuated Zn^{2+} accumulation induced by ischemia (Wang et al., 2010). Intracellular Zn^{2+} plays many physiological roles in cells (Bettger et al., 1981; Bray and Bettger, 1990; Cunningham-Rundles et al., 1990; Prasad 2009; Fukada et al., 2011). Therefore, it is important to characterize the changes in intracellular Zn^{2+} levels induced by clioquinol in order to reveal its toxicological profile, such that side effects can be avoided.

Toxicology studies of clioquinol in animals and humans reveal that the agent induces central and peripheral neurological symptoms, anemia, hepatotoxicity, and cardiovascular failure (Mao and Schimmer, 2008). When clioquinol is orally administrated, cells in both central and peripheral tissues are assumed to be affected. In this study, we mainly examined the effects of clioquinol on FluoZin-3 fluorescence, an indicator for intracellular Zn^{2+} level, in rat thymocytes in the presence and absence of extracellular Zn^{2+}. Rat thymocytes were used for the study for several reasons. Firstly, the cell membranes of thymocytes remain intact because single cells can be prepared without enzymatic treatment. Secondly, zinc plays a central role in the immune system and it is clear that zinc is crucial for the normal development and function of cells mediating immunity (Shankar and Prasad, 1998). The primary function of thymocytes is the maturation of T lymphocytes. The functions of T cells, i.e., recognizing foreign antigens, are mediated by T cell receptors. Finally, the modification of cell death (apoptosis and necrosis) by zinc has been studied extensively in murine thymocytes (Barbieri et al., 1992; McCabe et al., 1993; Provinciali et al., 1995; Maclean et al., 2001).

4.3.2. Clioquinol-induced changes in the intracellular Zn^{2+} concentration

FluoZin-3 fluorescence responds to changes in intracellular Zn^{2+} concentrations (Gee et al., 2002). Therefore, our results suggest that clioquinol increases the intracellular Zn^{2+} concentration in the presence of extracellular Zn^{2+} but decreases it in the absence of extracellular Zn^{2+}. This may be due to various reasons. Firstly, clioquinol, at concentrations ranging from 30 to 300 nM, augmented FluoZin-3 fluorescence in a concentration-dependent manner (Fig. 16B), suggesting that clioquinol increased the intracellular Zn^{2+} concentration in a concentration-dependent manner. Secondly, in the presence of DTPA, clioquinol, at concentrations ranging from 300 nM to 10 μM, attenuated FluoZin-3 fluorescence in a concentration-dependent manner (Fig. 19), suggesting that clioquinol decreased the intracellular Zn^{2+} concentration in a concentration-dependent manner. Clioquinol is membrane-permeable because of its lipophilic properties. Thus, when Zn^{2+} is present in the extracellular space, clioquinol seems to carry chelated Zn^{2+} into the cells, resulting in an increase in the intracellular Zn^{2+} level. Under the external Zn^{2+}-free conditions produced by DTPA, it is likely that clioquinol passes across the membranes and chelates the intracellular Zn^{2+}, resulting in a decrease in the intracellular Zn^{2+} level. The latter action of clioquinol was observed at micromolar concentrations. Micromolar concentrations of clioquinol may be excessive to chelate extracellular Zn^{2+}. Therefore, the action of clioquinol on FluoZin-3 fluorescence conformed to a bell-shaped curve in the absence of DTPA (Fig. 16B and Fig. 19B).

4.3.3. Augmentation of Fluo-3 fluorescence by clioquinol

Clioquinol at concentrations ranging from 30 nM to 300 nM increased the intensity of Fluo-3 fluorescence in a concentration-dependent manner (Fig. 18A). Fluo-3 fluorescence is also augmented by Zn^{2+} (Minta et al., 1989). Removal of external Zn^{2+} by DTPA, a chelator of Zn^{2+}, completely attenuated the clioquinol-induced augmentation of Fluo-3 fluorescence (Fig. 18B). Thus, the increase in intensity of Fluo-3 fluorescence by clioquinol was supposed to be due to the increase in intracellular Zn^{2+} concentration by clioquinol. It was unlikely that clioquinol at 30–300 nM increased intracellular Ca^{2+} concentration.

4.3.4. Toxicological implications

Zinc plays many physiological roles in cells and is required for the structure and function of proteins and cellular organelles (Bettger et al., 1981; Bray and Bettger, 1990; Cunningham-Rundles et al., 1990; Prasad 2009; Fukada et al., 2011). In mammalian immune cells, zinc is transported through the plasma membranes by zinc transporters of ZnT(SCL A30) or ZIP(SCL A39) families (Haase and Rink 2009). It cannot be ruled out the possibility that

clioquinol directly affects zinc transporters, leading to the changes in intracellular Zn^{2+} concentration. If clioquinol inhibits ZnT transporter or stimulates ZIP transport, the agent would increase intracellular Zn^{2+} concentration. However, there is no experimental evidence on the action of clioquinol on zinc transporters.

The increases in intracellular Zn^{2+} concentration have been detected under some stress conditions (Cima et al., 2006; Kinazaki et al., 2011). Zinc dyshomeostasis is recognized as an important mechanism for cellular malfunctions and cell death (Capasso et al., 2005; Kröncke, 2007). The effect of clioquinol on the intracellular Zn^{2+} level varied, depending on both the extracellular Zn^{2+} concentration and the clioquinol concentration, as shown in Fig. 16B, 17, and 19B. Clioquinol increased intracellular Zn^{2+} concentration in the presence of extracellular Zn^{2+}. Abnormal increases in intracellular Zn^{2+} concentrations have been associated with a variety of health problems (Frederickson et al., 2004; Maret and Sandstead, 2006; Cummings and Kovacic, 2009) and this may also be the case for clioquinol. If so, some of the side effects of clioquinol would be Zn^{2+}-dependent. In addition, one health implication can be extrapolated from our results. Many people use zinc supplementation in an attempt to affect the outcome of various diseases (Haase et al., 2008; Heyland et al., 2008). The combination of zinc supplements with lipophilic drugs that can chelate Zn^{2+} may disturb intracellular Zn^{2+} homeostasis.

4.4. CQ study-Part 2 – Clioquinol augments and attenuates the cytotoxicity of H_2O_2

4.4.1. Academic implication

Clioquinol, a lipophilic Zn^{2+} chelator, has emerged as a therapeutic metal-chelating agent for several diseases such as Alzheimer's disease and cancer. Clioquinol selectively binds to Zn^{2+}, and the binding affinity of clioquinol for Zn^{2+} is greater than that for Ca^{2+} (Cherny et al., 2001; Raman et al., 2005). Clioquinol can dissolve amyloid deposits because Zn^{2+} and Cu^{2+} are involved in the deposition and stabilization of amyloid plaques (Atwood et al., 2000; Curtain et al., 2001). Clinical trials have been performed using clioquinol for advanced hematologic malignancies and Alzheimer's disease (Ritchie et al., 2003; Lannfelt et al., 2008; Schimmer et al., 2012). Subacute myelo-optic neuropathy induced by clioquinol was an epidemic condition during the 1960s, which affected approximately 30,000 people in Japan (Takasu, 2003). Toxicological studies in animals and humans show that clioquinol induces central and peripheral neurological symptoms, anemia, hepatotoxicity, and cardiovascular failure (Mao and Schimmer, 2008). In addition, clioquinol affects the lymphocytes of patients with subacute myelo-optic neuropathy (Matsuda et al., 1991, 1994a, 1994b). Oral administration of clioquinol

affects the cells in the central and peripheral tissues.

In our previous study (Oyama et al., 2012), we determined the effect of clioquinol on intracellular Zn^{2+} levels in rat thymocytes to characterize the toxicological profile of clioquinol. We used rat thymocytes in this study for several reasons. The cell membranes of thymocytes remain intact because single cells can be obtained without enzymatic treatment. Further, zinc plays an important role in the immune system, and zinc is crucial for the normal development and function of cells that mediate immunity. Thymocytes play an important role in the maturation of T lymphocytes. The functions of T cells, i.e., recognition of foreign antigens, are mediated by T cell receptors. The change in the form of cell death (apoptosis and necrosis) by zinc has been extensively studied in murine thymocytes (Shanker et al., 1998; Barbieri et al., 1992). The concentration-response relationship of clioquinol-induced changes in intracellular Zn^{2+} levels of rat thymocytes showed a bell-shaped curve (Oyama et al., 2012). Clioquinol has different effects on the intracellular Zn^{2+} levels, and these effects depend on the extracellular Zn^{2+} concentrations and clioquinol concentrations. While extracellular application of zinc chloride ($ZnCl_2$) increases hydrogen peroxide (H_2O_2)-induced cytotoxicity, a chelator of intracellular Zn^{2+} attenuates this cytotoxicity (Matsui et al., 2010). Thus, intracellular Zn^{2+} is thought to be involved in the cell death induced by oxidative stress. Clioquinol can pass across the cell membranes and cause changes in intracellular Zn^{2+} levels; thus, it is important to examine the effects of clioquinol on oxidative stress-induced cell death under various conditions. Intracellular Zn^{2+} plays many physiological roles in regulating cellular functions (Bettger and O'Dell, 1981; Bray and Bettger, 1990; Cunningham-Rundles et al., 1990; Prasa, 2009; Fukuda et al., 2011); therefore, our study has several important implications. While clioquinol increases the intracellular Zn^{2+} concentration in some cell preparations (Andersson et al., 2009; Park et al., 2011), it decreases Zn^{2+} accumulation induced by ischemia (Wang et al., 2010). Changes in the intracellular Zn^{2+} levels modify the cytotoxicity of H_2O_2 (Matsui et al., 2010); thus, clioquinol may also modify oxidative stress-induced cytotoxicity, which is a common feature of almost all aerobic organisms that are capable of quenching reactive oxygen species to prevent their detrimental effects. To test this possibility, we examined the effects of clioquinol and Zn^{2+} chelators on cell death in response to H_2O_2-induced oxidative stress by using thymic lymphocytes and appropriate fluorescent probes.

4.4.2. Zn^{2+} dependence of clioquinol-induced potentiation of H_2O_2 cytotoxicity

Simultaneous incubation of cells with 300 μM H_2O_2 and clioquinol at concentrations ranging from 10 nM to 300 nM showed a bell-shaped profile of potentiation of H_2O_2

cytotoxicity (Fig. 20B). Maximum increase in cytotoxicity was observed at a concentration of 100 nM clioquinol, whereas 1 μM clioquinol decreased the cytotoxicity of H_2O_2. Clioquinol at a concentration of 100 nM increased the cytotoxicity of 30–300 μM H_2O_2 in a concentration-dependent manner (Fig. 20C). This increase in cytotoxicity may be dependent on clioquinol rather than on H_2O_2.

Although DTPA at a concentration of 10 μM did not affect the cytotoxicity of 300 μM H_2O_2 alone, DTPA significantly reduced the cytotoxicity induced by the combination of 300 μM H_2O_2 and 100 nM clioquinol (Fig. 22). DTPA significantly suppressed the transition of intact living cells to annexin V-positive living cells induced by the treatment with a combination of 300 μM H_2O_2 and 100 nM clioquinol (Fig. 21). TPEN at a concentration of 10 μM almost completely inhibited H_2O_2-induced cytotoxicity in the absence and presence of clioquinol (Fig. 22). Although extracellular Zn^{2+} is unlikely to be involved in the cytotoxicity induced by 300 μM H_2O_2 alone, clioquinol-induced increases in intracellular Zn^{2+} concentrations in the presence of extracellular Zn^{2+} seem to be a key factor in the increase in H_2O_2 cytotoxicity by clioquinol.

4.4.3. A possible mechanism underlying the bell-shaped concentration-response curve of clioquinol-induced changes in intracellular Zn^{2+} concentrations

We observed a bell-shaped concentration-response curve for increases in intracellular Zn^{2+} concentrations in the presence of extracellular Zn^{2+} induced by 30 nM to 3 μM clioquinol (Fig. 23A). This bell-shaped curve was also observed upon simultaneous treatment with 300 μM H_2O_2 and clioquinol (30 nM to 3 μM, Fig. 23B). Maximum increases in intracellular Zn^{2+} concentrations were observed with 300 nM clioquinol under both treatment conditions.

In the presence of 1 μM $ZnCl_2$, clioquinol further increased intracellular Zn^{2+} concentrations. However, the bell-shaped relationship between clioquinol concentration and FluoZin-3 fluorescence intensity became less apparent (Fig. 24A). On the other hand, under nominally Zn^{2+}-free conditions in the presence of DTPA, clioquinol at concentrations of 100 nM or more (up to 3 μM) decreased the intracellular Zn^{2+} levels in a concentration-dependent manner (Fig. 24B). Thus, the bell-shaped relationship is likely to be dependent on the concentrations of extracellular Zn^{2+} and clioquinol. Although Tyrode's solution lacks zinc salt, the cell suspension contained 200–230 nM Zn^{2+} derived from the cell preparation (Sakanashi et al., 2009). When the concentration of extracellular Zn^{2+} is greater than that of clioquinol, clioquinol may increase the intracellular Zn^{2+} levels in a concentration-dependent manner, presumably by membrane permeation of clioquinol with chelated Zn^{2+}. However, when the concentrations of extracellular

Zn^{2+} are less than those of clioquinol, both free and Zn^{2+}-chelated clioquinol may pass across the cell membranes, which results in a decrease in the intracellular Zn^{2+} concentrations compared to those in the controls or at peak levels.

4.4.4. Do clioquinol-induced increases in intracellular Zn^{2+} levels play a role in increasing H_2O_2 cytotoxicity?

The cytotoxicity induced by the combination of H_2O_2 and clioquinol was completely suppressed by TPEN (Fig. 21), which indicated that this effect was dependent on Zn^{2+}. The concentration of clioquinol required to elicit maximal increases in intracellular Zn^{2+} concentrations (Fig. 23) was different from that required to show a maximum increase in the cytotoxicity of H_2O_2 (Fig. 20B) although both concentration-response relationships showed a bell-shaped curve. While the increases in intracellular Zn^{2+} concentrations induced by treatment with a combination of 300 nM clioquinol and 300 μM H_2O_2 were greater than those induced by treatment with a combination of 100 nM clioquinol and 300 μM H_2O_2, cell death induced by the combination of 300 nM clioquinol and 300 μM H_2O_2 was lesser than that induced by 100 nM clioquinol and 300 μM H_2O_2. Therefore, in addition to the Zn^{2+}-chelating properties of clioquinol, clioquinol at concentrations ≥300 nM may have some cytoprotective actions against oxidative stress. The above finding was supported by our observation that clioquinol at concentrations ≥100 nM decreased the intensity of CM-DCF fluorescence (Fig. 25), a marker of cellular oxidant levels. The inconsistency between the results described in Figs. 20 and 23 have been explained on the basis of the inhibitory effect of clioquinol on oxidative stress at concentrations more than 100 nM (Fig. 25). However, these data may not be sufficient to support our findings because the inhibitory effect of clioquinol at 100 nM is almost the same as that at 300 nM, and clioquinol at 300 nM induced a maximum increase in the intracellular Zn^{2+} concentration. Therefore, this discrepancy may be explained on the basis of a mechanism other than that explained above. The cell death induced by H_2O_2 is dependent on the intracellular Zn^{2+} concentrations because TPEN, a membrane-permeable Zn^{2+} chelator, completely suppresses the H_2O_2-induced increase in cell lethality (Matsui et al., 2009). In addition, TPEN inhibits the increase in cell lethality induced by the combination of H_2O_2 and clioquinol. Zn^{2+} seems to be one of key elements in H_2O_2 cytotoxicity. Further, Ca^{2+} is involved in H_2O_2-induced cytotoxicity in rat thymocytes (Okazaki et al., 1996). Thus, both Ca^{2+} and Zn^{2+} are involved in H_2O_2-induced cytotoxicity. However, Zn^{2+} partly attenuates Ca^{2+}-dependent cell death (Sakanashi et al., 2009). The maximum increase in intracellular Zn^{2+} concentration by 300 nM clioquinol may inhibit the Ca^{2+}-dependent component of H_2O_2-induced cell death. The

bell-shaped response curve of Zn^{2+} was also observed in the Zn^{2+}-dependent augmentation of clotrimazole cytotoxicity (Oyama et al., 2007). In addition, high concentrations of Zn^{2+} may have an inhibitory effect on Ca^{2+}-dependent cell death induced by H_2O_2.

Previous studies (Matsui et al., 2009; Kinazaki et al., 2011) showed that the application of micromolar $ZnCl_2$ increased the lethality of cells simultaneously incubated with H_2O_2, although zinc is known to act as an antioxidant (Bray and Bettger, 1990; Powell, 2000). H_2O_2 itself significantly increased the intracellular Zn^{2+} concentration. Thus, the intracellular Zn^{2+} concentration markedly increased with the combination of clioquinol and H_2O_2. Micromolar zinc inhibits respiratory chain in the mitochondria (Skulachev et al., 1967; Nicholls and Malviya, 1968). Cultured neurons exposed to high concentrations of Zn^{2+} develop mitochondrial failure that is dependent on the zinc concentration (Manev et al., 1997). Furthermore, zinc irreversibly damages major enzymes of energy production (Gararyan et al., 2007) prior to zinc-dependent multi-conductance channel activity in mitochondria (Bonanni et al., 2006). Therefore, the increase in the intracellular Zn^{2+} concentration because of the combination of H_2O_2 and clioquinol may induce malfunction of mitochondria in this cell preparation, which results in necrosis or apoptosis (Lemasters et al., 1999). In addition, an excessive increase in intracellular Zn^{2+} concentration may change the intracellular oxidative state. Zn^{2+} and ascorbate together promote lipid peroxidation in the brain membranes (Diaz-Arrastia and Hashemi, 2000). This effect is unique to Zn^{2+}, and other divalent cations do not share similar synergism with ascorbic acid. If rat thymocytes possess sufficient levels of ascorbate, intracellular Zn^{2+}-ascorbate interaction may be one of the mechanisms for the cytotoxicity induced by clioquinol and H_2O_2.

In addition, our study showed that clioquinol a lipophilic Zn^{2+}-chelating compound increased the intracellular Zn^{2+} concentrations under certain in vitro conditions. Clioquinol may exert diverse Zn^{2+}-dependent effects because of the following reasons: Zn^{2+} has many physiological and pathological roles such as in maintaining membrane plasticity, cell injury, and cell death (Sensi et al., 2011). Intracellular Zn^{2+} homeostasis is regulated by Zn^{2+} transporters, Na^+-Zn^{2+} and H^+-Zn^{2+} exchangers, Zn^{2+}-importing proteins, and Zn^{2+}-buffering peptides such as metallothionein (Maret, 2009; Ohana et al., 2009). Excessive increase in intracellular Zn^{2+} concentration by clioquinol presumably induces intracellular Zn^{2+} dyshomeostasis that may lead to pathophysiological changes in cellular functions.

4.5. Aspects of Environmental and regional sciences in present in vitro toxicological study

We show that the chemical has Zn^{2+}-dependent cytotoxicity, suggesting that the

cytotoxicity of chemical substances is enhanced in the presence of Zn^{2+}. There are many chemical substances around us, and their cytotoxicity may develop because of coexistence with Zn^{2+}. The related concerns of note are as follows. Emissions from activities such as metal mining, inorganic pigment manufacturing, inorganic chemical industrial product manufacturing, surface-treated steel manufacturing, and electroplating, are a considerable source of environmental zinc exposure (Harte et al., 1991; Gakwisiri et al., 2012). According to the provisions in the Water Pollution Control Law in Japan, the permissible zinc levels of wastewater from business establishments are set at 2 mg/L or lower (calculated molar concentration: 30.6 μM). Zinc levels in river water are 0.14–19.7 mg/L in the Przemsza River of Poland (Pistelok and Galas, 1999), 0.71–1.76 mg/L in the Gombak River and Penchala River of Malaysia (Ismail et al., 2013), and 4.2–6.7 mg/L in the Godavari River of India (Sayyed and Bhosle, 2010). When converted to molar concentrations, the levels are in the range of 2.1–301.3 μM. In our study, $ZnCl_2$ at 30 μM markedly potentiated the cytotoxicity of PS80 in vitro (Fig. 4). In addition, the cytotoxicity of the antimicrobial CTZ is enhanced by 0.3–10 μM $ZnCl_2$ (Oyama et al., 2007). These in vitro concentrations of $ZnCl_2$ are lower than the levels in river water, but they still potentiated the cytotoxicity of some chemical compounds. Thus, zinc is a critical factor that must be taken into consideration with regard to environmental conservation (or protection). Zn^{2+} enhances the cytotoxicity of imidazole fungicides, but not triazole fungicides (Matsui et al., 2008). The former compounds increase intracellular Zn^{2+} concentration but the latter do not. Therefore, it is necessary to consider the chemicophysical properties of compounds that may increase membrane Zn^{2+} permeability or form a membrane-permeable complex with Zn^{2+}. Triclosan is one such environmental pollutant; it is an antibacterial agent present in healthcare products such as hand soap and toothpaste, as well as in urban river water worldwide. Triclosan has also been detected in river water in Tokushima City. The involvement of Zn^{2+} in the cytotoxicity of triclosan has previously been demonstrated (Tamura et al., 2012). The concentration of zinc in the river water of Tokushima City is 0.005 mg/L, which is not a problematic level. However, the zinc concentration of river sediments varies depending on the geology and deposits in the area. Regional distribution of each element is shown in the geochemical map as important, basic, national information at the National Geological Survey Center of National Institute of Advanced Industrial Science and Technology. Therefore, it is necessary to manage chemical substances with zinc levels in river water and sediments in the future.

5. Acknowledgment

I would like to appreciate the members of my thesis committee at Graduate School of Integrated Arts and Sciences, Tokushima University: Professor Kumio Yokoigawa, Professor Tatsuo Hamano, and Associate Professor Takehumi Hattori for their insightful comments and encouragement. My sincere thanks also go to Professor Yoshiro Okano (Tokushima Bunri University and Daiichi University of Pharmacy), Professor Yasuo Oyama (Tokushima University), Associate Professor Shiro Ishida (Tokushima Bunri University), Professor Hakaru Seo (Sojo University), and Professor Hitoshi Ishibashi (Kitasato University) who provided me an opportunity to conduct my research.

References

Ak, T., Gülçin, I., 2008. Antioxidant and radical scavenging properties of curcumin. Chem. Biol. Interact. 174, 27-37.

Andersson, D.A., Gentry, C., Moss, S., Bevan, S., 2009. Clioquinol and pyrithione activate TRPA1 by increasing intracellular Zn^{2+}. Proc. Natl. Acad. Sci. USA. 106, 8374–8379.

Antizar-Ladislao, B., 2008. Environmental levels, toxicity and human exposure to tributyltin (TBT)-contaminated marine environment. a review. Environ. Int. 34, 292-308.

Atwood, C.S., Scarpa, R.C., Huang, X., Moir, R.D., Jones, W.D., Fairlie, D.P., Tanzi, R.E., Bush, A.I., 2000. Characterization of copper interactions with Alzheimer amyloid β peptides: Identification of an attomolar-affinity copper binding site on amyloid β1-42. J. Neurochem. 75, 1219–1233.

Bae, S,N,, Kim, J., Lee, Y.S., Kim, J.D., Kim, M.Y., Park, L.O., 2007. Cytotoxic effect of zinc-citrate compound on choriocarcinoma cell lines. Placenta. 28, 22-30.

Bae, S.N., Lee, Y.S., Kim, M.Y., Kim, J.D., Park, L.O., 2006. Antiproliferative and apoptotic effects of zinc-citrate compound (CIZAR(R)) on human epithelial ovarian cancer cell line, OVCAR-3. Gynecol. Oncol. 103, 127-136.

Baker, S.D., Zhao, M., He, P., Carducci, M.A., Verweij, J., Sparreboom, A., 2004. Simultaneous analysis of docetaxel and the formulation vehicle polysorbate 80 in human plasma by liquid chromatography/tandem mass spectrometry. Anal. Biochem. 324, 276-284.

Banni, M., Chouchene, L., Said, K., Kerkeni, A., Messaoudi, I., 2011. Mechanisms underlying the protective effect of zinc and selenium against cadmium-induced oxidative stress in zebrafish Danio rerio. Biometals. DOI: 10.1007/s10534-011-9456-z

Bao, V.W., Leung, K.M., Kwok, K.W., Zhang, A.Q., Lui, G.C., 2008. Synergistic toxic effects of zinc pyrithione and copper to three marine species: Implications on setting appropriate water quality criteria. Mar. Pollut. Bull. 57, 616-623.

Barbieri, D., Troiano, L., Grassilli, E., Agnesini, C., Cristofalo, E.A., Monti, D., Capri, M.,

Cossarizza, A., Franceschi, C., 1992. Inhibition of apoptosis by zinc: A reappraisal. Biochem. Biophys. Res. Comm. 187, 1256-1261.

Barnett, B.L., Kretschmar, H.C., Hartman, F.A., 1977. Structural characterization of bis(N-oxopyridine-2-thionato)zinc(II). Inorg. Chem., 16, 1834-1838.

Beauvai, F., Michel, L., Dubertret, L., 1995. Human eosinophils in culture undergo a striking and rapid shrinkage during apoptosis. Role of K^+ channels. J. Leuko. Biol. 57, 851-855.

Beaver, J.P., Waring, P., 1995. A decrease in intracellular glutathione concentration precedes the onset of apoptosis in murine thymocytes. Eur. J. Cell Biol. 68, 47-54.

Bellas, J., 2005. Toxicity assessment of the antifouling compound zinc pyrithione using early developmental stages of the ascidian Ciona intestinalis. Biofouling. 21, 289-296.

Bellas, J., Granmo, K., Beiras, R., 2005. Embryotoxicity of the antifouling biocide zinc pyrithione to sea urchin (Paracentrotus lividus) and mussel (Mytilus edulis). Mar. Pollut. Bull. 50, 1382-1385.

Benzie, I.F., 2000. Evolution of antioxidant defence mechanisms. Eur. J. Nutr. 39, 53–61.

Bettger, W.J., O'Dell, B.L., 1981. A critical physiological role of zinc in the structure and function of biomembranes. Life Sci. 28, 1425–1438.

Bolognin, S., Drago, D., Messori, L., Zatta, P., 2009. Chelation therapy for neurodegenerative diseases. Med. Res. Rev. 29, 547–570.

Bonanni, L., Chachar, M., Jover-Mengual, T., Li, H., Jones, A., Yokota, H., Ofengeim, D., Flannery, R.J., Miyawaki, T., Cho, C.H., Polster, B.M., Pypaert, M., Hardwick, J.M., Sensi, S.L., Zukin, R.S., Jonas E.A., 2006. Zinc-dependent multi-conductance channel activity in mitochondria isolated from ischemic brain. J. Neurosci. 26, 6851–6862.

Bortner, C.D., Cidlowski, J.A., 1998. A necessary role for cell shrinkage in apoptosis. Biochem. Pharmacol. 56, 1549-1559.

Bray, T.M., Bettger, W.J., 1990. The physiological role of zinc as an antioxidant. Free Radic. Biol. Med. 8, 281–291.

Brown, K.H., 1998. Effect of infections on plasma zinc concentration and implications for zinc

status assessment in low-income countries. Amer. J. Clin. Nutri. 68, 425S-429S.

Cabreiro, F., Picot, C.R., Perichon, M., Friguet, B., Petropoulos, I., 2009. Overexpression of methionine sulfoxide reductases A and B2 protects MOLT-4 cells against zinc-induced oxidative stress. Antioxid. Redox. Signal. 11, 215-225.

Cai, L., Li, X.K., Song, Y., Cherian, M.G., 2005. Essentiality, toxicology and chelation therapy of zinc and copper. Curr. Med. Chem. 12, 2753–2763.

Calgaroto, N.S., Cargnelutti, D., Rossato, L.V., Farias, J.G., Nunes, S.T., Tabaldi, L.A., Antes, F.G., Flores, E.M., Schetinger, M.R., Nicoloso, F.T., 2011. Zinc alleviates mercury-induced oxidative stress in Pfaffia glomerata (Spreng.) Pedersen. Biometals. 24, 959-971.

Capasso, M., Jeng, J.M., Malavolta, M., Mocchegiani, E., Sensi, S.L., 2005. Zinc dyshomeostasis: a key modulator of neuronal injury. J. Alzheimers Dis. 8, 93–108.

Cherny, R.A., Atwood, C.S., Xilinas, M.E., Gray, D.N., Jones, W.D., McLean, C.A., Barnham, K.J., Volitakis, I., Fraser, F.W., Kim, Y., Huang, X., Goldstein, L.E., Moir, R.D., Lim, J.T., Beyreuther, K., Zheng, H., Tanzi, R.E. Masters, C.L., Bush, A.I., 2001. Treatment with a copper-zinc chelator markedly and rapidly inhibits beta-amyloid accumulation in Alzheimer's disease transgenic mice. Neuron. 30, 665–676.

Chikahisa, L., Oyama, Y., 1992. Tri-n-butyltin increases intracellular Ca^{2+} in mouse thymocytes: a flow-cytometric study using fluorescent dyes for membrane potential and intracellular Ca^{2+}. Pharmacol. Toxicol. 71, 190-195.

Chikahisa, L., Oyama, Y., Okazaki, E., Noda, K., 1996. Fluorescent estimation of H_2O_2-induced changes in cell viability and cellular nonprotein thiol level of dissociated rat thymocytes. Jpn. J. Pharmacol. 71, 299-305.

Chikahisa, L., Oyama, Y., Okazaki, E., Noda, K., 1996. Fluorescent estimation of H_2O_2-induced changes in cell viability and cellular nonprotein thiol level of dissociated rat thymocytes. Jpn. J. Pharmacol. 71, 299–305.

Choyke, P.L., Zeman, R.K., Gootenberg, J.E., Greenberg, J.N., Hoffer, F., Frank, J.A., 1987.

Thymic atrophy and regrowth in response to chemotherapy: CT evaluation. Amer. J. Roentgenol. 149, 269-272.

Chukhlovin, A.B., Tokalov, S.V., Yagunov, A.S., Westendorf, J., Reincke, H., Karbe, L., 2001. In vitro suppression of thymocyte apoptosis by metal-rich complex environmental mixtures: potential role of zinc and cadmium excess. Sci. Total Environ. 281, 153-163.

Chung, M.K., Han, S.S., Kim, J.C., 2006. Evaluation of the toxic potentials of a new camptothecin anticancer agent CKD-602 on fertility and early embryonic development in rats. Regul. Toxicol. Pharmacol. 45, 273-281.

Cima, R.R., Dubach, J.M., Wieland, A.M., Walsh, B.M., Soybel, D.I., 2006. Intracellular Ca^{2+} and Zn^{2+} signals during monochloramine-induced oxidative stress in isolated rat colon crypts. Am. J. Physiol. Gastrointest. Liver Physiol. 290, G250–261.

Cortese, M.M., Suschen, K., Wetzel, W., Kroncke, K.D., Kolb-Bachofenm V., 2008. Zinc protects endothelial cells from hydrogen peroxide via Nrf2-dependent stimulation of glutathione biosynthesis. Free Radic. Biol. Med. 44, 2002-2012.

Cummings, J.E., Kovacic, J.P., 2009. The ubiquitous role of zinc in health and disease. J. Vet. Emerg. Crit. Care (San Antonio). 19, 215–240.

Cunningham-Rundles, S., Bockman, R.S., Lin, A., Giardina, P.V., Hilgartner, M.W., Caldwell-Brown, D., Carter, D.M., 1990. Physiological and pharmacological effects of zinc on immune response. Ann. N. Y. Acad. Sci., 587, 113–122.

Curtain, C.C., Ali, F., Volitakis, I., Cherny, R.A., Norton,, R.S., Beyreuther, K., Barrow, C.J., Masters, C.L., Bush, A.I., Barnham, K.J., 2001. Alzheimer's disease amyloid-β binds copper and zinc to generate an allosterically ordered membrane-penetrating structure containing superoxide dismutase-like subunits. J. Biol. Chem., 276, 20466–20473.

Daniel, K.G., Chen, D., Orlu, S., Cui, Q.C., Miller, F.R., Dou, Q.P., 2005. Clioquinol and pyrrolidine dithiocarbamate complex with copper to form proteasome inhibitors and apoptosis inducers in human breast cancer cells. Breast Cancer Res. 7, R897–908.

Diaz-Arrastia, R., Hashemi, E., 2000. Zinc and ascorbic acid coordinately promote lipid

peroxidation in brain membranes. J. Mol. Neurosci. 14, 167–173.

Diaz-Cruz, M.S., Mendiete, J., Monjonell, A., Tauler, R., Esteban, M., 1998. Study of the zinc-binding properties of glutathione by differential pulse polarography and multivariate curve resolution. J. Inorg. Biochem. 70, 91-98.

Dickinson, B.C., Chang, C.J., 2011. Chemistry and biology of reactive oxygen species in signaling or stress responses. Nature Chem. Biol. 7, 504-511.

Ebdon, L., Evans, K., Hill, S., 1989. The accumulation of organotins in adult and seed oysters from selected estuaries prior to the introduction of U.K. regulations governing the use of tributyltin-based antifouling paints. Sci. Total Environ. 83, 63-84.

Engels, F.K., Mathot, R.A., Verweij, J., 2007. Alternative drug formulations of docetaxel: a review. Anticancer Drugs 18, 95-103.

Farinati, F., Cardin, R., D'inca, R., Naccarato, R., Sturniolo, G.C., 2003. Zinc treatment prevents lipid peroxidation and increases glutathione availability in Wilson's disease. J. Lab. Clin. Med. 141, 372-377.

Figueiredo-Pereira, M.E., Cohen, G., 1999. The ubiquitin/proteasome pathway: friend or foe in zinc-, cadmium-, and H_2O_2-induced neuronal oxidative stress. Mol. Biol. Rep. 26, 65-69.

Fink, B., Laude, K., McCann, L., Doughan, A., Harrison, D.G., Dikalov, S., 2004. Detection of intracellular superoxide formation in endothelial cells and intact tissues using dihydroethidium and an HPLC-based assay. Am. J. Physiol. Cell Physiol. 287, C895-C902.

Fong, L.Y., Nguyen, V.T., Farber, J.L., 2001. Esophageal cancer prevention in zinc-deficient rats: rapid induction of apoptosis by replenishing zinc. J. Nati. Cancer Instit. 93, 1525-1533.

Franklin, R.B., Costello, L.C., 2007. Zinc as an anti-tumor agent in prostate cancer and in other cancers. Archi. Biochem. Biophys. 463, 211-217.

Frederickson, C.J., Maret, W., Cuajungco, M.P., 2004. Zinc and excitotoxic brain injury: a new model. Neuroscientist. 10, 18–25.

Fukada, T., Yamasaki, S., Nishida, K., Murakami, M., Hirano, T., 2011. Zinc homeostasis and

signaling in health and diseases: Zinc signaling. J. Biol. Inorg. Chem. 16, 1123–1134.

Gabathuler, R., 2010. Approaches to transport therapeutic drugs across the blood-brain barrier to treat brain diseases. Neurobiol. Disease. 37, 48-57.

Gee, K.R., Zhou, Z.L., Qian, W.J. Kennedy, R., 2002. Detection and imaging of zinc secretion from pancreatic beta-cells using a new fluorescent zinc indicator. J. Am. Chem. Soc. 124, 776–778.

Gelinsky, M., Vogler, R., Vahrenkamp, H., 2003. Zinc complexation of glutathione and glutathione-derived peptides. Inorg. Chimica Acta 344, 230-238.

Gelperina, S.E., Khalansky, A.S., Skidan, I.N., Smirnova, Z.S., Bobruskin, A.I., Severin, S.E., Turowski, B., Zanella, F.E., Kreuter, J., 2002. Toxicological studies of doxorubicin bound to polysorbate 80-coated poly(butyl cyanoacrylate) nanoparticles in healthy rats and rats with intracranial glioblastoma. Toxicol. Lett. 126, 131-141.

Gibson, W.T., Chamberlain, M., Parsons, J.F., Brunskill, J.E., Leftwich, D., Lock, S., Safford, R.J., 1985. The effect and mode of action of zinc pyrithione on cell growth. I. In vitro studies. Food Chem. Toxicol. 23, 93-102.

Giustarini, D., Dalle-Donne, I., Tsikas, D., Rossi, R., 2009. Oxidative stress and human diseases: Origin, link, measurement, mechanisms, and biomarkers. Crit. Rev. Clin. Lab. Sci. 46, 241-281.

Goka, K., 1999. Embryotoxicity of zinc pyrithione, an antidandruff chemical, in fish. Environ. Res. 81, 81-83.

Gracia, R.C., Snodgrass, W.R., 2007. Lead toxicity and chelation therapy. Am. J. Health Syst. Pharm. 64, 45–53.

Gruver, A.L., Sempowski, G.D., 2008. Cytokines, leptin, and stress-induced thymic atrophy. J. Leuko. Biol. 84, 915-923.

Gulyaev, A.E., Gelperina, S.E., Skidan, I.N., Antropov, A.S., Kivman, G.Y., Kreuter, J., 1999. Significant transport of doxorubicin into the brain with polysorbate 80-coated nanoparticles. Pharmaceut. Res. 16, 1564-1569.

Guthery, E., Seal, L.A., Anderson, E.L., 2005. Zinc pyrithione in alcohol-based products for skin antisepsis: persistence of antimicrobial effects. Am. J. Infect. Control. 33, 15-22.

Ha, K.N., Chen, Y., Cai, J., Sternberg, P.Jr., 2006. Increased glutathione synthesis hrough on ARE-Nrf2-dependent pathway by zinc in the RPE: Implication for protection against oxidative stress. Invest. Ophthalmol. Visual Sci. 47, 2709-2715.

Haase, H., Overbeck, S., Rink, L., 2008. Zinc supplementation for the treatment or prevention of disease: current status and future perspectives. Exp. Gerontol. 43, 394–408.

Haase, H., Rink, L., 2009. The immune system and the impact of zinc during aging. Immun. Ageing 6:9.

Hashimoto, E., Oyama, T.B., Oyama, K., Nishimura, Y., Oyama, T.M., Ueha-Ishibashi, T., Okano, Y, Oyama, Y., 2009. Increase in intracellular Zn^{2+} concentration by thimerosal in rat thymocytes: intracellular Zn^{2+} release induced by oxidative stress. Toxicol. In Vitro 23, 1092-1099.

Hayes, J.D., McLellan, L.I., 1999. Glutathione and glutathione-dependent enzymes represent a co-ordinately regulated defence against oxidative stress. Free Radic. Res. 31, 273-300.

Hegde, M.L., Bharathi, P., Suram, A., Venugopal, C., Jagannathan, R., Poddar, P., Srinivas, P., Sambamurti, K., Rao, K.J., Scancar, J., Messori, L., Zecca, L., Zatta, P., 2009. Challenges associated with metal chelation therapy in Alzheimer's disease. J. Alzheimers. Dis. 17, 457–468.

Hendrickx, P.H., Dohring, W., 1989. Thymic atrophy and rebound enlargement following chemotherapy for testicular cancer. Acta Radiologica. 30, 263-267.

Heyland, D.K., Jones, N., Cvijanovich, N.Z., Wong, H., 2008. Zinc supplementation in critically ill patients: a key pharmaconutrient? J. Parenter. Enteral. Nutr. 32, 509–519.

Hirama, S., Tatsuishi, T., Iwase, K., Nakao, H., Umebayashi, C., Nishizaki, Y., Kobayashi, M., Ishida, S., Okano, Y., Oyama, Y., 2004. Flow-cytometric analysis on adverse effects of polysorbate 80 in rat thymocytes. Toxicol. 199, 137-143.

Hjorth, M., Dahllöf, I., Forbes, V.E., 2006. Effects on the function of three trophic levels in

marine plankton communities under stress from the antifouling compound zinc pyrithione. Aquat .Toxicol. 77, 105-115.

Jacob, C., Maret, W., Valle, B.L., 1998. Control of zinc transfer between thionein, metallothionein, and zinc proteins. Proc. Nati. Acad. Sci. U.S.A. 95, 3489-3494.

Jaiswal, A.S., Narayan, S., 2004. Zinc stabilizes adenomatous polyposis coli (APC) protein levels and induces cell cycle arrest in colon cancer cells. J. Cell. Biochem. 93, 345-357.

Jiang, L.J., Maret, W., Vallee, B.L., 1998. The glutathione redox couple modulates zinc transfer from metallothionein to zinc-depleted sorbitol dehydrogenase. Proc. Nati. Acad. Sci. U.S.A. 95, 3483-3488.

Jin, Z., El-Deiry, W.S., 2005. Overview of cell death signaling pathways. Cancer Biol. Ther. 4, 139–163.

Jomova, K., Valko, M., 2011. Advances in metal-induced oxidative stress and human disease. Toxicol. 283, 65-87.

Kao, J.P., Harootunian, A.T., Tsien, R.Y., 1989. Photochemically generated cytosolic calcium pulses and their detection by fluo-3. J. Biol. Chem. 264, 8179–8184.

Kasi, V., Bodiga, S., Kommuguri, U.N., Sankuru, S., Bodiga, V.L., 2011. Zinc pyrithione salvages reperfusion injury by inhibiting NADPH oxidase activation in cardiomyocytes. Biochem. Biophys. Res. Commun. 410, 270-275.

Kawanai, T., Satoh, M., Murao, K., Oyama, Y., 2009. Methylmercury elicits intracellular Zn^{2+} release in rat thymocytes: Its relation to methylmercury-induced decrease in cellular thiol content. Toxicol. Lett. 191, 231–235.

Kimura, K., Nishimura, Y., Oyama, K., Kawanai, T., Hashimoto, E., Oyama, Y., 2011. Tetracaine decreases intracellular Zn^{2+} concentration by inhibiting Zn^{2+} influx in rat thymocytes. Nat. Sci. Res. Univ. Tokushima 25, 7-13.

Kinazaki, A., Chen, H., Koizumi, K., Kawanai, T., Oyama, T.M., Satoh, M., Ishida, S., Okano, Y., Oyama, Y., 2011. Putative role of intracellular Zn^{2+} release during oxidative stress: a trigger to restore cellular thiol content that is decreased by oxidative stress. J. Physiol. Sci.

61, 403–409.

Klassen, N.V., Walker, P.R., Ross, C.K., Cygler, J., Lach, B., 1993. Two-stage cell shrinkage and the OER for radiation-induced apoptosis of rat thymocytes. Intl. J. Rad. Biol. 64, 571-581.

Konstantinou, I.K., Albanis, T.A., 2004. Worldwide occurrence and effects of antifouling paint booster biocides in the aquatic environment: a review. Environ. Int. 30, 235-348.

Koopman, G., Reutelingsperger, C.P., Kuijten, G.A., Keehnen, R.M., Pals, S.T., van Oers, M.H. 1994. Annexin V for flow cytometric detection of phosphatidylserine expression on B cells undergoing apoptosis. Blood. 84, 1415-1420.

Koopman, W.J., Verkaart, S., van Emst-de Vries, S.E., Grefte, S., Smeitink, J.A., Willems, P.H., 2007. Simultaneous quantification of oxidative stress and cell spreading using 5-(and-6)-chloromethyl-2',7'-dichlorofluorescein. Cytometry A. 69, 1184–1192.

Kröncke, K.D., 2007. Cellular stress and intracellular zinc dyshomeostasis. Arch. Biochem. Biophys. 463, 183–187.

Kumar, A., Malhotra, A., Nair, P., Garg, M., Dhawan, D.K., 2010. Protective role of zinc in ameliorating arsenic-induced oxidative stress and histological changes in rat liver. J. Environ. Pathol. Toxicol. Oncol. 29, 91-100.

Kumari, A., Yadav, S.K., Yadav, S.C., 2010. Biodegradable polymeric nanoparticles based drug delivery systems. Coll. Surf. B: Biointerefaces 75, 1-18.

Lamore, S.D., Wondrak, G.T., 2011. Zinc pyrithione impairs zinc homeostasis and upregulates stress response gene expression in reconstructed human epidermis. Biometals. 24, 875-890.

Lannfelt, L., Blennow, K., Zetterberg, H., Batsman, S., Ames, D., Harrison, J., Masters, C.L., Targum, S., Bush, A.I., Murdoch, R., Wilson, J., Ritchie, C.W., 2008. Safety, efficacy, and biomarker findings of PBT2 in targeting Aβ as a modifying therapy for Alzheimer's disease: a phase IIa, double-blind, randomised, placebo-controlled. Lancet Neurol. 7, 779–786.

Lemasters, J.J., Qian, T., Bradham, C.A., Brenner, D.A., Cascio, W.E., Trost, L.C., Nishimura,

Y., Nieminen, A.L., Herman, B., 1999. Mitochondrial dysfunction in the pathogenesis of necrotic and apoptotic cell death. J. Bioenerg. Biomembr. 31, 305–319.

Lin, A.M., Chen, K.B., Chao, P.L., 2005. Antioxidative effect of vitamin D3 on zinc-induced oxidative stress in CNS. Ann. N.Y. Acad. Sci. 1053, 319-329.

Loos, W.J., Baker, S.D., Verweij, J., Boonstra, J.G., Sparreboom, A., 2003. Clinical pharmacokinetics of unbound docetaxel: role of polysorbate 80 and serum proteins. Clin. Pharmacol. Therapeu. 74, 364-371.

Macho, A., Hirsch, T., Marzo, I., Marchetti, P., Dallaporta, B., Susin, S.A., Zamzami, N., Kroemer, G., 1997. Glutathione depletion is an early and calcium elevation is a late event of thymocyte apoptosis. J. Immunol. 158, 4612-4619.

Maclean, K.H., Cleveland, J.L., Porter, J.B., 2001. Cellular zinc content is a major determinant of iron chelator-induced apoptosis of thymocytes. Blood. 98, 3831–3839.

Manev, H., Kharlamov, E., Uz, T., Mason, R.P., Cagnoli, C.M., 1997. Characterization of zinc-induced neuronal death in primary cultures of rat cerebellar granule cells. Exp. Neurol. 146, 171–178.

Mann, J.J., Fraker, P.J., 2005. Zinc pyrithione induces apoptosis and increases expression of Bim. Apoptosis. 10, 369-379.

Mao, X., Schimmer, A.D., 2008. The toxicology of clioquinol. Toxicol. Lett. 182, 1–6.

Maraldo, K., Dahllöf, I., 2004. Indirect estimation of degradation time for zinc pyrithione and copper pyrithione in seawater. Mar. Pollut. Bull. 48, 894-901.

Marcheselli, M., Azzoni, P., Mauri, M., 2011. Novel antifouling agent-zinc pyrithione: stress induction and genotoxicity to the marine mussel Mytilus galloprovincialis. Aquat. Toxicol. 102, 39-47.

Marcheselli, M., Conzo, F., Mauri, M., Simonini, R., 2010a. Novel antifouling agent—zinc pyrithione: short- and long-term effects on survival and reproduction of the marine polychaete Dinophilus gyrociliatus. Aquat. Toxicol. 98, 204-210.

Marcheselli, M., Rustichelli, C., Mauri, M., 2010b. Novel antifouling agent zinc pyrithione:

determination, acute toxicity, and bioaccumulation in marine mussels (Mytilus galloprovincialis). Environ. Toxicol. Chem. 29, 2583-2592.

Maret, W., 1994. Oxidative metal release from metallothionein via zinc-thiol/disulfide interchange. Proc. Nat. Acad. Sci. U.S.A. 91, 237-241.

Maret, W., 2009. Molecular aspects of human cellular zinc homeostasis: redox control of zinc potentials and zinc signals. Biometals. 22, 149–157.

Maret, W., Sandstead, H.H., 2006. Zinc requirements and the risks and benefits of zinc supplementation. J. Trace Elem. Med. Biol. 20, 3–18.

Maret, W., Vallee, B.L., 1998. Thiolate ligands in metallothionein confer redox activity on zinc clusters. Proc. Nati. Acad. Sci. U.S.A. 95, 3478-3482.

Marks, R., Pearse, A.D., Walker, A.P., 1985. The effects of a shampoo containing zinc pyrithione on the control of dandruff. Br. J. Dermatol. 112, 415-422.

Matsuda, M., Miyagi, K., Yanagisawa, N., Tsukada, N., 1994. Age-related changes of B-cell immune function in patients with subacute mtelo-optico-neuropathy (SMON) [Article in Japanese], Arerugi, 43, 1215-1219.

Matsuda, M., Yanagisawa, N., Tsukada, N., 1991. Subsets of peripheral blood lymphocytes and ageing in patients with SMON [Article in Japanese], Arerugi, 40, 1226-1231.

Matsui, H., Oyama, T.M., Okano, Y., Hashimoto, E., Kawanai, T. Oyama, Y., 2010. Low micromolar zinc exerts cytotoxic action under H_2O_2-induced oxidative stress: excessive increase in intracellular Zn^{2+} concentration. Toxicol., 276, 27–32.

Matsui, H., Sakanashi, Y., Nishimura, Y., Kawanai, T., Oyama, Y., Ishida, S., Okano, Y., 2009. Effects of Zn^{2+} chelators, DTPA and TPEN, and $ZnCl_2$ on the cells treated with hydrogen peroxide: a flow-cytometric study using rat thymocytes. Nat. Sci. Res. (Univ. Tokushima) 23, 12–18.

Matsui, H., Sakanashi, Y., Oyama, T.M., Oyama, Y., Yokota, S., Ishida, S., Okano, Y., Oyama, T.B., Nishimura, Y., 2008. Imidazole antifungals, but not triazole antifungals, increase membrane Zn^{2+} permeability in rat thymocytes: Possible contribution to their cytotoxicity.

Toxicol. 248, 142-150.

McCabe Jr, M.J., Jiang, S.A., Orrenius, S., 1993. Chelation of intracellular zinc triggers apoptosis in mature thymocytes. Lab. Invest. 69, 101–110.

McConkey, D.J., Jondal, M., Orrenius, S., 1994. The regulation of apoptosis in thymocytes. Biochem. Soc. Transac. 22, 606-610.

McMillian, M., Nie, A., Parker, J.B., Leone, A., Kemmerer, M., Bryant, S., Herlich, J., Yieh, L., Bittner, A., Liu, X., Wan, J., Johnson, M.D., Lord, P., 2005. Drug-induced oxidative stress in rat liver from a toxicogenomics perspective. Toxicol. Appl. Pharmacol. 207, 171-178.

Messaoudi, I., Hammouda, F., El Heni, J., Baati, T., Saïd, K., Kerkeni, A., 2010. Reversal of cadmium-induced oxidative stress in rat erythrocytes by selenium, zinc or their combination. Exp. Toxicol. Pathol. 62, 281-288.

Migliore, L., Coppedè, F., 2009. Environmental-induced oxidative stress in neurodegenerative disorders and aging. Mutat. Res. 674, 73-84.

Minta, A., Kao, J.P., Tsien, R.Y., 1989. Fluorescent indicators for cytosolic calcium based on rhodamine and fluorescein chromophores. J. Biol. Chem. 264, 8171–8178.

Morina, F., Jovanovic, L., Mojovic, M., Vidovic, M., Pankovic, D., Veljovic Jovanovic, S., 2010. Zinc-induced oxidative stress in Verbascum thapsus is caused by an accumulation of reactive oxygen species and quinhydrone in the cell wall. Physiol. Plant. 140, 209-224.

Nagano, T., Oyama, Y., Kajita, N., Chikahisa, L., Nakata, M., Okazaki, E., Masuda, T., 1997. New curcuminoids isolated from Zingiber cassumunar protect cells suffering from oxidative stress: a flow-cytometric study using rat thymocytes and H_2O_2. Jpn. J. Pharmacol. 75, 363-370.

Nakata, M., Oyama, Y., Okada, Y., Yamazaki, Y., Chikahisa, L., Satoh, M., 1999. Flow cytometric analysis on tri-n-butyltin-induced increase in annexin V binding to membranes of rat thymocytes. Environ. Toxicol. Pharmacol. 7, 267-273.

National Toxicology Program, 1992. Toxicology and carcinogenesis studies of polysorbate 80 (CAS No. 9005-65-6) in F344/N rats and B6C3F1 mice (Feed studies). Nat. Toxicol.

Program Technical Report Series 415, 1-225.

Nicholls, P., Malviya, A.N., 1968. Inhibition of nonphosphorylating electron transfer by zinc. The problem of delineating interaction sites. Biochem. 7, 305–310.

Oberle, R.L., Moore, T.J., Krummel, D.A., 1995. Evaluation of mucosal damage of surfactants in rat jejunum and colon. J. Pharmacol. Toxicol. Meth. 33, 75-81.

Ohana, E., Hoch, E., Keasar, C., Kambe, T., Yifrach, O., Hershfinkel, M., Sekler, I., 2009. Identification of the Zn^{2+} binding site and mode of operation of a mammalian Zn^{2+} transporter. J. Biol. Chem. 284, 17677–17686.

Okazaki, E., Chikahisa, L., Kanemaru, K., Oyama, Y., 1996. Flow cytometric analysis of the H2O2-induced increase in intracellular Ca2+ concentration of rat thymocytes. Jpn. J. Pharmacol. 71, 273–280.

Oyama, T.B., Oyama, K., Kawanai, T., Oyama, T.M., Hashimoto, E., Satoh, M., Oyama, Y., 2009. Tri-n-butyltin increases intracellular Zn^{2+} concentration by decreasing cellular thiol content in rat thymocytes. Toxicol. 262, 245-249.

Oyama, T.M., Ishida, S., Okano, Y., Seo, H., Oyama, Y., 2012. Clioquinol-induced increase and decrease in the intracellular Zn^{2+} level in rat thymocytes. Life Sci. 91, 1216–1220.

Oyama, T.M., Saito, M., Yonezawa, T., Okano, Y., Oyama, Y., 2012. Nanomolar concentrations of zinc pyrithione increase cell susceptibility to oxidative stress induced by hydrogen peroxide in rat thymocytes. Chemosphere. 87, 1316–1322.

Oyama, Y., Masuda, T., Nakata, M., Chikahisa, L., Yamazaki, Y., Miura, K., Okagawa, M., 1998. Protectice actins of 5'-n-alkylated curcumins on living cells suffering from oxidative stress. Eur. J. Pharmacol. 360, 65-71.

Oyama, Y., Matsui, H., Morimoto, M., Sakanashi, Y., Nishimura, Y., Ishida, S., Okano, Y., 2007. Synergic cytotoxic action induced by simultaneous application of zinc and clotrimazole in rat thymocytes. Toxicol. Lett. 171, 138–145.

Oyama, Y., Noguchi, S., Nakata, M., Okada, Y., Yamazaki, Y., Funai, M., Chikahisa, L. Kanemaru K., 1999. Exposure of rat thymocytes to hydrogen peroxide increases annexin V

binding to membranes: inhibitory actions of deferoxamine and quercetin. Eur. J. Pharmacol. 384, 47–52.

Park, M.H., Lee, S.J., Byun, H.R., Kim, Y., Oh, Y.J., Koh, J.Y., Hwang, J.J., 2011. Clioquinol induces autophagy in cultured astrocytes and neurons by acting as a zinc ionophore. Neurobiol. Dis. 42, 242–251.

Pellegrini, M., Baldari, C.T., 2009. Apoptosis and oxidative stress-related diseases: the p66Shc connection. Curr. Mol. Med. 9, 392-398.

Powell, S.R., 2000. The antioxidant properties of zinc. J. Nutr. 130, 1447S–154S.

Prasad, A.S., 1995. Zinc: an overview. Nutrition. 11, 93-99.

Prasad, A.S., 2009. Zinc: role in immunity, oxidative stress and chronic inflammation. Curr. Opin. Clin. Nutr. Metab. Care. 12, 646–652.

Priestley, G.C., Brown, J.C., 1980. Acute toxicity of Zinc pyrithione to human skin cells in vitro. Acta. Derm. Venereol. 60, 145-148.

Provinciali, M., Di Stefano, G., Fabris, N., 1995. Dose-dependent opposite effect of zinc on apoptosis in mouse thymocytes. Int. J. Immunopharmacol. 17, 735-744.

Quaglino, D., Ronchetti, I.P., 2001. Cell death in the rat thymus: a minireview. Apoptosis. 6, 389-401.

Quesada, A.R., Bymes, R.W., Krezoski, S.O., Petering, D.H., 1996. Direct reaction of H_2O_2 with sulfhydrlyl groups in HL-60 cells: Zinc-metallothionein and other sites. Arch. Biochem. Biophys. 334, 241-250.

Raman, B., Ban. T., Yamaguchi, K.I., Sakai, M., Kawai, T., Naiki, H., Goto, Y., 2005. Metal ion-dependent effects of clioquinol on the fibril growth of an amyloid β peptide. J. Biol. Chem., 280, 16157–16162.

Rege, B.D., Kao, J.P., Polli, J.E., 2002. Effects of nonionic surfactants on membrane transporters in Caco-2 cell monolayers. Euro. J. Pharmaceut. Sci. 16, 237-246.

Ritchie, C.W., Bush, A.I., Mackinnon, A., Macfarlane, S., Mastwyk, M., MacGregor ,L., Kiers, L., Cherny, R., Li, Q.X., Tammer, A., Carrington, D., Mavros, C., Volitakis, I., Xilinas, M.,

Ames, D., Davis, S,, Beyreuther, K., Tanzi, R.E., Masters, C.L., 2003. Metal-protein attenuation with iodochlorhydroxyquin (clioquinol) targeting a β amyloid deposition and toxicity in Alzheimer disease: a pilot phase 2 clinical trial. Arch. Neurol., 60, 1685–1691.

Romieu, I., Castro-Giner, F., Kunzli, N., Sunyer, J., 2008. Air pollution, oxidative stress and dietary supplementation: a review. Eur. Respir. J. 31, 179-197.

Rudolf, E., Cervinka, M., 2010. Zinc pyrithione induces cellular stress signaling and apoptosis in Hep-2 cervical tumor cells: the role of mitochondria and lysosomes. Biometals. 23, 339-354.

Rudolf, E., Cervinka, M., 2011. Stress responses of human dermal fibroblasts exposed to zinc pyrithione. Toxicol. Lett. 204, 164-173.

Sakanashi, Y., Oyama, T.M., Matsuo, Y., Oyama, T.B., Nishimura, Y., Ishida, S., Imai, S., Okano, Y., Oyama, Y., 2009. Zn^{2+}, derived from cell preparation, partly attenuates Ca^{2+}-dependent cell death induced by A23187, calcium ionophore, in rat thymocytes. Toxicol. In Vitro. 23, 338-345.

Sampson, B., Kovar, I.Z., Rauscher, A., Fairweather-Tait, S., Beattie, J., McArdle, H.J., Ahmed, R., Green, C., 1997. A case of hyperzincemia with functional zinc depletion: a new disorder? Pedia. Res. 42, 219-225.

Sandstead, H.H., 1994. Understanding zinc: recent observations and interpretations. J. Lab. Clin. Med. 124, 322-327.

Schimmer, A.D., Jitkova, Y., Gronda, M., Wang, Z., Brandwein, J., Chen, C., Gupta, V., Schuh, A., Yee, K., Chen, J., Ackloo, S., Booth ,T., Keays, S., Minden, M.D., 2012. A phase I study of the metal ionophore clioquinol in patients with advanced hematologic malignancies. Clin. Lymphoma Myeloma Leuk. 12, 330–336.

Sensi, S.L., Paoletti, P., Koh, J.Y., Aizenman, E., Bush, A.I., Hershfinkel, M., 2011. The neurophysiology and pathology of brain zinc. J. Neurosci. 31, 16076–16085.

Shankar, A.H., Prasad, A.S., 1998. Zinc and immune function: the biological basis of altered resistance to infection. Am. J. Clin. Nutr. 68, 447S-463S.

Singh, B.K., Kumar, A., Ahmad, I., Kumar, V., Patel, D.K., Jain, S.K., Singh, C., 2011. Oxidative stress in zinc-induced dopaminergic neurodegeneration: Implications of superoxide dismutase and heme oxygenase-1. Free Radic. Res. 45, 1207-1222.

Singh, C., Ahmad, I., Kumar, A., 2007. Pesticides and metals induced Parkinson's disease: involvement of free radicals and oxidative stress. Cell. Mol. Biol. 53, 19-28.

Sirmali, M., Uz, E., Sirmali, R., Kilbaş, A., Yilmaz, H.R., Altuntaş, I., Naziroğlu, M., Delibaş, N., Vural, H., 2007. Protective effects of erdosteine and vitamins C and E combination on ischemia-reperfusion-induced lung oxidative stress and plasma copper and zinc levels in a rat hind limb model. Biol. Trace Elem. Res. 118, 43-52.

Skulachev, V.P., Chistyakov, V.V., Jasaitis, A.A., Smirnova, E.G., 1967. Inhibition of the respiratory chain by zinc ions. Biochem. Biophys. Res. Commun. 26, 1–6.

Sunderman, F.W.Jr., 1995. The influence of zinc on apoptosis. Ann Clin Lab Sci. 25, 134-142.

Takasu, T., 2003. SMON – a model of iatrogenic disease [Article in Japanese], Rinsho Shikeigaku, 43, 866-869.

Tatsuishi, T., Oyama, Y., Iwase, K., Yamaguchi, J.Y., Kobayashi, M., Nishimura, Y., Kanada, A., Hirama, S., 2005. Polysorbate 80 increases the susceptibility to oxidative stress in rat thymocytes. Toxicol. 207, 7-14.

Thoman, C.J., 1999. The versatility of polysorbate 80 (Tween 80) as a ionophore. J. Pharmaceut. Sci. 88, 258-260.

Tije, A.J.T., Verweij, J., Loos, W.J., Sparreboom, A., 2003. Pharmacological effects of formulation vehicles: implications for cancer chemotherapy. Clin. Pharmacokinet. 42, 665-685.

Tsujino, I., Yamazaki, T., Masutani, M., Sawada, U., Horie, T., 1999. Effect of Tween-80 on cell killing by etoposide in human lung adenocarcinoma cells. Cancer Chemother. Pharmacol. 43, 29-34.

Varghese, J., Faith, M., Jacob, M., 2009. Zinc prevents indomethacin-induced renal damage in rats by ameliorating oxidative stress and mitochondrial dysfunction. Eur. J. Pharmacol. 614,

114-121.

Vermes, I., Haanen, C., Steffens-Nakken, H., Reutelingsperger, C., 1995. A novel assay for apoptosis. Flow cytometric detection of phosphatidylserine expression on early apoptotic cells using fluorescein labelled Annexin V. J. Immunol. Meth. 184, 39-51.

Wang, T., Zheng, W., Xu, H., Zhou, J.M., Wang, Z.Y., 2010. Clioquinol inhibits zinc-triggered caspase activation in the hippocampal CA1 region of a global ischemic gerbil model. PLoS One. 5, e11888.

Warner, R.R., Schwartz, J.R., Boissy, Y., Dawson, T.L.Jr., 2001. Dandruff has an altered stratum corneum ultrastructure that is improved with zinc pyrithione shampoo. J. Am. Acad. Dermatol. 45, 897-903.

Webster, L.K., Linsenmeyer, M.E., Rischin, D., Urch, M.E., Woodcock, D.M., Millward, M.J., 1997. Plasma concentrations of polysorbate 80 measured in patients following administration of docetaxel or etoposide. Cancer Chemother. Pharmacol. 39, 557-60.

Wuehler, S.E., Sempértegui, F., Brown, K.H., 2008. Dose-response trial of prophylactic zinc supplements, with or without copper, in young Ecuadorian children at risk of zinc deficiency. Amer. J. Clin. Nutri. 87, 723-733.

Yang, Y., Ashwell, J.D., 1999. Thymocyte apoptosis. J. Clin. Immunol. 19, 337-349.

Zalewski, P.D., Forbes, I.J., Giannakis, C., 1991. Physiological role for zinc in prevention of apoptosis (gene-directed death). Biochem. Internat. 24, 1093-1101.